Review

How Chemoresistive Sensors Can Learn from Heterogeneous Catalysis. Hints, Issues, and Perspectives

Jessica Yazmín Monter-Guzmán [1], Xiangfeng Chu [2], Elisabetta Comini [3], Mauro Epifani [4],* **and Rodolfo Zanella [1],***

[1] Instituto de Ciencias Aplicadas y Tecnología, Universidad Nacional Autónoma de México, Circuito Exterior S/N, C.U., México City 04510, Mexico; jessyiq0410@gmail.com

[2] School of Chemistry and Chemical Engineering, Anhui University of Technology, Maanshan 243002, China; xfchu99@ahut.edu.cn

[3] Department of Information Engineering, Brescia University, Via Valotti 9, 25133 Brescia, Italy; comini@sensor.ing.unibs.it

[4] Istituto per la Microelettronica e i Microsistemi, IMM-CNR, Via Monteroni, 73100 Lecce, Italy

* Correspondence: maurosalvatore.epifani@cnr.it (M.E.); rodolfo.zanella@icat.unam.mx (R.Z.)

Abstract: The connection between heterogeneous catalysis and chemoresistive sensors is emerging more and more clearly, as concerns the well-known case of supported noble metals nanoparticles. On the other hand, it appears that a clear connection has not been set up yet for metal oxide catalysts. In particular, the catalytic properties of several different oxides hold the promise for specifically designed gas sensors in terms of selectivity towards given classes of analytes. In this review, several well-known metal oxide catalysts will be considered by first exposing solidly established catalytic properties that emerge from related literature perusal. On this basis, existing gas-sensing applications will be discussed and related, when possible, with the obtained catalysis results. Then, further potential sensing applications will be proposed based on the affinity of the catalytic pathways and possible sensing pathways. It will appear that dialogue with heterogeneous catalysis may help workers in chemoresistive sensors to design new systems and to gain remarkable insight into the existing sensing properties, in particular by applying the approaches and techniques typical of catalysis. However, several divergence points will appear between metal oxide catalysis and gas-sensing. Nevertheless, it will be pointed out how such divergences just push to a closer exchange between the two fields by using the catalysis knowledge as a toolbox for investigating the sensing mechanisms.

Keywords: metal oxide gas sensors; surface modification; heterogeneous catalysis

1. Introduction

It is customary to introduce additives to metal oxide-based chemosensors in order to enhance such features as the response magnitude and selectivity. Such additives are very often constituted by noble metals in various forms [1]; their use finds its physicochemical foundation in heterogeneous catalysis, specifically in the concept of spillover [2,3]. Yamazoe systematized the predicted effects of noble metals additives on chemosensors by also introducing the concept of electronic sensitization [4]. It is not surprising that such a connection exists between heterogeneous catalysis and chemosensors. Clearly, if a material features specific catalytic capabilities to oxidize/convert a given gaseous species, the basis is posed to desirable sensing behavior, with the condition that such surface reactions can be rapidly and efficiently translated, by the material itself, into appropriate electronic response. It is not straightforward to meet this condition, and the huge number of papers about this topic clearly shows the complexity of the task, including the need for tools that suitably tackle the involved reaction mechanisms. Still, the way is shown to try and draw from heterogeneous catalysis, possibly even in a direction

beyond the classical addition of noble metals. In this review, the concept of metal oxide heterogeneous catalysis will be elaborated as a fruitful crossroad with the chemosensors field. This development will be conducted by reviewing various metal oxide catalytic systems that will be shown to be of potential interest even to chemoresistive sensors. On the other hand, points of divergence between the two research fields will also be indicated in order to avoid unjustified analogies but also to show how catalysis may help to improve research methodology in oxide chemosensors.

2. What Can Be Expected from Further Interaction with Metal Oxide Heterogeneous Catalysis

In the field of chemoresistive sensors, looking at catalysis is an early phenomenon. The first commercial sensors, the Figaro family of products, are routinely prepared by Pd addition to the SnO_2 active materials [5]. Since then, sensors where noble metals have been added to a metal oxide have been deeply investigated as concerns the sensing mechanisms [6,7]. Moreover, their connection with catalysis has been clearly outlined [1]. Therefore, the case of noble metal additives will not be considered in the following. Instead, we will try to show that the exchange between *metal oxide* heterogeneous catalysis and chemoresistive oxide sensors can be very fruitful too. This happens because the connection between the two fields is profound beyond the case of noble metals, even though it is often overlooked. In heterogeneous catalysis, one is interested in converting a known reactant into a product at the maximum possible rate using the mildest possible conditions, minimizing the catalyst amount, and working with the largest possible reactant feedstock. In chemoresistive sensors, the analyte is in principle unknown and is typically present in ppm/ppb concentrations. For this reason, the aim of a sensing device is to maximize the electronic outcome of the sensing reaction(s): obtaining readable electrical signal in the presence of, in principle, even a single electronic exchange between the gas and the sensing layer. This result can be obtained if the sensing materials can transform the reaction with the analyte molecules into electrical charges as fast and efficiently as it can, hence, if it is an efficient catalyst for some specific reaction. Therefore, we switch from heterogeneous catalysis to chemoresistive sensing by simply focusing our attention onto what happens electronically to the catalytic support (placed into a suitable readout circuit) instead of what happens chemically to the gaseous analyte. If a sensing material is not capable of catalyzing any useful (i.e., resulting in appreciable electronic modification of the material itself) reaction, it can hardly be a good performing sensor. Instead, an efficient catalyst may be a good sensor. Many requirements must be met for obtaining such a result. The most trivial requirement is that the sensor materials must not be an insulator. For this reason, well-known catalysts composed by insulating supports, such as Al_2O_3 and SiO_2, will not be considered in the following. Another condition is that the catalyzed reaction must be able to provide a clear electronic outcome. For instance, good candidates are oxidation (combustion) reactions, which consume surface and/or bulk oxygen anions from the catalyst, obviously resulting in conductance changes (oxygen chemisorption/consumption occur at the expense of the sensor charges). Furthermore, the reaction kinetics must not be too sluggish; otherwise, it may be contrasted by other ongoing reactions (for instance, oxygen re-adsorption). Finally, it must not be neglected that the surface species involved in the conductance change cannot be the same involved in catalytic reactions with the same material [8]. It is not straightforward at all to provide a precise prediction on the basis of these conditions. However, it should be now clear that, by properly perusing even the metal oxide catalysis field, potentially good sensors can be suggested. In the following, we propose an example of such an approach. The catalytic metal oxides are partially taken from recent reviews [9–13]. Metal oxide catalysts for the *combustion* of Volatile Organic Compounds (VOCs) will be considered in particular. On the contrary, extensive lists of known sensing applications have recently been published [14,15]. By cross-referencing such lists and similar ones, we discuss, in the following, the possible sensors-catalysis connections by inspecting in closer detail several well-established material typologies. What will emerge is also a series of expectable

discrepancy points between metal oxide catalysis and gas sensors. We will try to evidence that these discrepancies can actually become a stimulus to tackle the gas-sensing challenges with an enriched perspective.

3. A Selection of Case Studies

Before proceeding, we will clarify the following points for the reader's convenience:

As stated before, the addition of noble metals and the formation of oxide–oxide nanocomposites will not be reviewed, focusing the attention on the catalytic properties of single metal oxides as such;

When possible, a summarizing scheme will be included in each section for easing the comparison between catalysis and sensing results. Given the difference in the two kinds of experiments, the "best performance" temperature seemed the only affordable parameter to collect the data (we avoid the term "compare the data" since it would be rather undefined in the present context);

We are not going to compile an extensive list of material and/or applications. In each case, several excellent specific reviews are available, as referred to in the text. Therefore, the present work should be seen as a collection of important and indicative results to constitute a stimulus to workers in the field of gas-sensors to draw from metal oxide catalysis.

The results will be presented by referring to Table 1 in an order going from p to n semiconductors.

Table 1. The left column reports examples of catalyzed reactions by the metal oxides reported in the adjacent column. The right column reports known and suggested and/or scarcely explored (cell below the dashed line) sensing applications.

Catalyzed Reactions	Composition	Sensing Application
CO oxidation, total oxidation of 2-propanol, ethanol, formaldehyde, toluene, methane, and ammonia	Co_3O_4	CO, ethanol, ammonia, isopropanol toluene
		Apart for CO and ethanol, the other applications deserve further developments.
Combustion of toluene, benzene, ethanol, and methane; formaldehyde and CO oxidation	$MnO*_x$	H_2, ethanol, acetone
		Methane (possibly at high temperatures)
CO oxidation	CuO	Ethanol, CO, acetone, formaldehyde, benzene, H_2S
CO oxidation, total oxidation of toluene, and formaldehyde and methane combustion	NiO	ethanol
		CO, toluene, acetone, formaldehyde
CO oxidation, total oxidation of toluene, ethyl acetate, acetaldehyde, and various hydrocarbons	Cr_2O_3	H_2, ethanol, toluene, formaldehyde
		CO, hydrocarbons, ethyl acetate,
CO oxidation, total oxidation of methane, ethanol, ethyl acetate, benzene, toluene, acetone, isopropanol, etc.	Perovskites (ABO_3 general composition)	Methanol, ethanol, ammonia, alkanes, H_2S, SO_2, acetylene
		Benzene, toluene, acetone, formaldehyde
CO oxidation, total oxidation of methane, propane, toluene	Fe_2O_3	Acetone, ethanol, butanol, H_2S
		CO, Methane, propane, toluene
Total oxidation of chlorobenzenes and benzene; partial oxidation of o-xylene and of methanol; oxidative dehydrogenation of propane	TiO_2-V_2O_5	Ethanol, acetone
		Benzene, toluene, chlorobenzenes, alkanes
Oxidation of CO, ethylene, propene, propane; oxidation of o-xylene and 2-propanol	SnO_2-V_2O_5	
		Benzene and derivatives, alkanes and other hydrocarbons, alcohols
Isopropanol dehydration, cyclopentene oxidation	TiO_2-WO_3	Acetone, ethanol
		Alcohols, hydrocarbons
Partial oxidation of methanol and ethanol; dehydrosulfurization and ammoxidation reactions	TiO_2-MoO_3	CO, acetone
		Alcohols, H_2S, other sulfur compounds, benzene, and derivatives

*: see text for a distinction among Mn oxide phases.

3.1. Co$_3$O$_4$

Co$_3$O$_4$, a p-type semiconductor featuring the normal spinel structure, has been attracting attention as a gas sensor for long time [16]. It is a good candidate for clarifying the concept of catalysis related to sensing properties due to several applications in both fields.

Co$_3$O$_4$ is a well-known catalyst for CO oxidation [11]. In very dry conditions, CO oxidation was reported at −54 °C [17] and, more recently, at −77 °C in humid air using nanorods [18]. In the presence of 3 ppm H$_2$O, the combustion was complete at about 40 °C. In humid conditions (6000 ppm H$_2$O), the total conversion of CO occurred at higher temperatures; however, it was complete at 150 °C [17]. The low operating temperatures and the influence of humidity in the atmosphere are interesting common points with gas-sensing, as evidenced in 2013 by the Tubingen group [19]. The authors reported a very large response to both CO (50 ppm, the response was almost two orders of magnitude in dry air, about 2 at 50% RH) and ethanol (90 ppm, the response was almost three orders of magnitude in dry air, about 10 at 50% RH), even without noble metal additives at as low as a 100 °C operating temperature. Therefore, the initial suggestion from catalysis (Co$_3$O$_4$ as CO sensor) resulted in really powerful sensors at remarkably low-operating temperatures. A remarkable spread exists, however, in the data reported in the literature for CO sensing. For instance, Deng et al. [20] reported a response of about 8.5 to 50 ppm CO at 180 °C.

The recently established total oxidation of 2-propanol by Co$_3$O$_4$ at 150 °C confirms its aptitude for VOC sensing [21], as recently confirmed for 2-propanol itself (about a 250% response at 275 °C, 10 ppm concentration) [22]. A relationship between Co$_3$O$_4$ catalytic activity toward alcohol oxidation and sensing properties had indeed already been suggested in 2010 [23], where ethanol sensing was investigated. A response of 57.7 was obtained toward 100 ppm ethanol at an operating temperature of 400 °C using Co$_3$O$_4$ nanosheets. The operating temperature is in agreement with recent results about ethanol complete combustion over Co$_3$O$_4$ at 350 °C [24]. A remarkable spread of sensing results can be observed in the case of ethanol too. For instance, Lü et al. [25] reported a response of about 3.5 to 200 ppm ethanol at about 350 °C by concave Co$_3$O$_4$ nanocubes, while Jiao et al. reported a response of about 15 at 180 °C to 100 ppm ethanol with Co$_3$O$_4$ microspheres. Co$_3$O$_4$ is also known as a catalyst for methane [11], propane (T$_{90}$ = 250 °C) [26], and other alkanes combustion. The use of Co$_3$O$_4$ nanosheets led to the almost complete combustion of methane at about 360 °C [27]. However, very low responses (about 1 at 100 °C operating temperature for 500 ppm methane concentration) were found in the few published papers concerning such sensing applications [19,28]. Moreover, the response was negligible in the presence of 50% RH in both references. The similar behavior toward humidity is an indication of common reaction mechanisms on the Co$_3$O$_4$ surface. Due to the different synthesis processes, this observation is consistent with a methane-sensing mechanism different from the catalytic pathway, probably involving different oxygen species.

Co$_3$O$_4$ is an interesting catalyst for formaldehyde oxidation [29]. The authors reported the total consumption of formaldehyde at room temperature by Co$_3$O$_4$ nanobelts. This result could suggest Co$_3$O$_4$ as an interesting material for formaldehyde sensing, too. In fact, for instance, Kim et al. [30] prepared hollow Co$_3$O$_4$ spheres by template method. They obtained an appreciable response (about 8) to as low as 800 ppb formaldehyde concentration. It is important to observe that, in general agreement with many other reports, interestingly low operating temperatures, such as 150 °C, could be applied for obtaining the best response. This result is in agreement with the observed low-temperature catalytic activity of Co$_3$O$_4$.

The total oxidation of toluene [31] by Co$_3$O$_4$ was reported at temperatures ranging from 250 to 300 °C. On the other hand, toluene sensors with the best operating temperatures ranging around 200 °C (10 to 100 ppm concentrations, response from about 6 to 7) have been published [16]. Ammonia is a peculiar and instructive case. While a response of 11.2 was reported to 100 ppm NH$_3$ concentration [32] at as low as a 160 °C operating temperature, ammonia oxidation by CO$_3$O$_4$ required very high temperatures around 700 °C [33].

Ammonia, with its complex reaction mechanisms, is a typical case where different surface species may be involved in each process. It further invites us to be cautious and avoid the straightforward conclusion from the other results in Figure 1 that sensing and catalysis follow parallel pathways. It is, however, clear that the sensing operation is almost invariably convenient at low temperatures, and that, in general, both applications provide the best performances at comparably low operating temperatures. With this precaution in mind, we now turn our attention to another material characterized by varied catalytic properties but not deeply investigated yet as gas-sensor, manganese oxides.
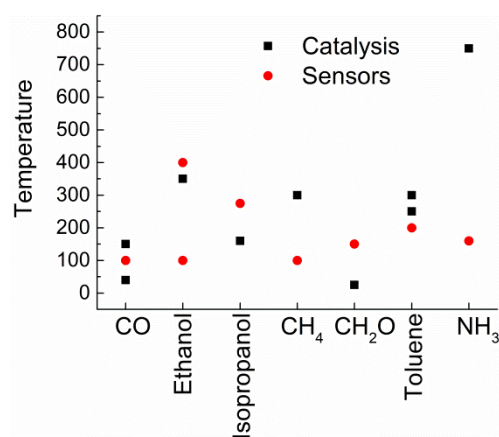
Figure 1. Best operating temperatures for the indicated sensing (best operating temperature and response tradeoff) and oxidation (lowest total combustion temperature) experiments over Co_3O_4 materials. More points are present when appreciable spread of the results was found. The references are reported in the discussion.

Summarizing with the help of Figure 1, we have found that a closely parallel behavior can be observed, with the typical operating temperatures that rarely span an interval over 150–200 °C. Remarkable differences can be seen between methane and ammonia. It is due to the high stability of methane and the complex reaction mechanisms of ammonia, a fact that will be observed in several other examples below. However, the doubts exposed in ref. [19] that concern the effectively operating sensing mechanisms must be taken into account.

3.2. Manganese Oxides

In this paragraph, we present a unified discussion of the various Mn oxides used in catalysis since it is customary to find many different phases tested for the same reaction. The described materials typically behave as p-type semiconductors, so they can be of interest as chemoresistive gas sensors. Of the several phases formed by manganese when combined with oxygen, Mn_3O_4, Mn_2O_3 and MnO_2 are of particular interest here. The last one has been reported to feature about 14 different crystallographic phases [34–36], which explains the difficulty in understanding the catalytic mechanisms. However, the catalytic properties of Mn oxides are of remarkable interest for possible sensing applications due to the broad range of VOCs that can be oxidized. Kim et al. [37] found that the catalytic activities toward the oxidation of toluene and benzene were in the order α-Mn_3O_4 > α-Mn_2O_3 > β-MnO_2, with a T_{90} (the temperature for achieving 90% conversion) of 270 °C for Mn_3O_4. Lamaita et al. [38] found total ethanol combustion at 200 °C with a sample constituted by γ-MnO_2 (nsutite). Practically all of the six commonly found phases for MnO_2 have been tested for formaldehyde oxidation, an extensive review of which has been published [39]. Interestingly, the compiled T_{100} (the temperature for achieving total conversion) values did not surpass 200 °C, which is a very useful feature for low power consumption sensors. Similar observations can be drawn from a more recent review [40]. β-MnO_2 was found by Li et al. [41] as the most active phase toward CO oxidation with a T_{90} of 109 °C. In the case of Mn oxides, the relationship with sensing applications is not very

well defined, very few sensing papers having been published. Bigiani et al. investigated the H_2 sensing properties of α-Mn_3O_4, which provided very low responses in the absence of noble metal promoters (less than 10% at 300 °C for 200 ppm concentration) [42]. More interesting responses were obtained toward ethanol (50 ppm, response almost 150 at 300 °C) and acetone (100 ppm, response more than 150 at 300 °C) [43], which was in agreement with those obtained by Lee and coworkers [44] for 100 ppm ethanol concentration. δ-MnO_2 was shown to be an interesting sensor for H_2 traces (response of about 4 to 50 ppm H_2 at 200 °C) [45]. The methane combustion was reported by several Mn oxides [46], but it required rather high temperatures (>723 K); therefore, it can be assumed to not be very attractive for low power consumption sensors.

On the basis of these results, it seems that the potential sensing capabilities of Mn oxides have not been fully exploited yet, and a number of gas targets are suggested in Table 1 as possibly interesting analytes to be explored.

3.3. CuO and NiO

These two p-type semiconductors are treated together since they share some common features: (i) they are mostly known as catalysts for CO oxidation; (ii) the range of sensing applications is much broader than CO and includes several different analytes. CuO is a very well-known catalyst for an ample range of organic syntheses [47], but, when dealing with gas–solid heterogeneous catalysis, it is moderately active towards CO oxidation in an unsupported form: "In comparison to Co_3O_4, unsupported copper oxides have been more rarely used in CO oxidation. This is essentially due to the typical structure of cobalt oxide, which contains both Co^{2+} and Co^{3+}, whereas CuO or Cu_2O have only either Cu^{2+} or Cu^+ ions" [48]. However, Zedan et al. have reported that, depending on the pre-treatment of CuO nanoparticles, the complete conversion of CO can be obtained at as low an operating temperature of 125 °C [49]. CuO is much more active as a supported catalyst, but the support is generally alumina or ceria, which are not suitable for chemoresistive sensing. Despite the limited range of catalytic applications of unsupported CuO, several examples of CuO-based sensors can be found in the literature [50,51]. It is worth mentioning a few of the results. Zhang and coworkers [52] reported 50 ppm benzene sensing at 230 °C with CuO octahedral nanoparticles (response was 9.7), with interesting selectivity with respect to toluene and ethylbenzene. Lee et al. established 250 °C as the best operating temperature for detecting down to 50 ppb formaldehyde by CuO nanocubes (response was about 1) [53]. Sowwan and coworkers could detect down to 1 ppm CO at 325 °C, with a response of 6.4%, by using CuO nanowires directly grown onto hotplates [54]. Wang et al. [55] reported sensing of ethanol, acetone and methanol down to 0.1 ppm concentrations at 220 °C (responses ranging from about 2 to 2.5) Important performances as concerns H_2S sensing have been reported recently by Li et al. [56]. The authors could report a response of 0.5 to 0.5 ppb H_2S concentration at room temperature. Therefore, CuO is a case where sensing applications remarkably enlarge the catalysis targets. Moreover, the catalysis and gas-sensing results are not easily composed into a unitary view. While catalytic properties are enhanced by depositing the catalyst onto support, several gases could be detected by pure CuO in several forms, as mentioned above. This could be an indication that, such as for Co_3O_4, gas-sensing and catalysis may follow different surface reaction pathways.

The catalytic oxidation of CO by NiO has been known for a long time [57]. In that work, oxygen species that adsorbed onto vacant surface sites were supposed to be responsible for CO oxidation at low temperatures (<180 °C). Accordingly, in a recent work, the oxygen species generated by its interaction with unsaturated surface Ni cations were considered responsible for CO oxidation [58]. Such availability of active, surface oxygen species seems very promising for sensing applications. Further catalytic applications of unsupported NiO include formaldehyde (total mineralization at 90 °C over mesoporous NiO) [59], toluene oxidation ($T_{90\%}$ = 242 °C for 500 ppm [60] or 300 °C for 1000 ppm [61]), and methane combustion [62], even though, for the latter, it occurred at high temperatures (complete conversion at 460 °C). On this basis, several sensing applications can be expected from

NiO-based devices. Indeed, a perusal of NiO-related reviews [63,64] indicates that many different analytes have been already tested. Recent examples of ethanol sensing include the use of NiO nanosheets [65] and nanoflowers [66], resulting in responses of, respectively, 65 to to 50 ppm ethanol at 250 °C and of 40 to 200 ppm of ethanol at 300 °C. NiO as acetone-sensing material has seldom been considered. Liu et al. [67] detected 17 ppm of acetone at 350 °C with a response below 2. More recently, Urso et al. have used NiO nanowalls for detecting down to 10 ppm acetone at 250 °C with a 30% response [68]. Very few examples are available concerning formaldehyde sensing. An important case is the paper by Castro-Hurtado et al., where modeling of the sensing properties was also attempted [69]. The authors detected 5 ppm of formaldehyde at about 350 °C with a response of 2. The authors established that oxygen species were adsorbed onto the material surface, favored by the Ni^{2+}-Ni^{3+} equilibrium, and then acted as reactive sites for formaldehyde molecules, even at 50 °C. Then, even CO [70] and toluene [67] seem interesting examples of target gases that are not yet fully explored by NiO (very few data have been published to date). Actually, much of the literature focuses on the modification of NiO with various additives; therefore, it is difficult to assess the sensing potential of the pure material.

Nevertheless, this seems an important case study to be further developed, where fundamental studies are needed in order to assess the influence of oxygen vacancies on surface chemistry. Despite a rather sparse distribution of studies about catalytic and sensing properties, Figure 2 allows us to highlight some trends. First of all, it can be seen that some sensing applications are missing (methane), which might be discouraged because of the high operating temperatures required by such gas. In other cases, there are very few sensing studies in the literature, in agreement with the above-mentioned preference for NiO modified with additives. Above all, a general trend is observed where gas sensors are operated at higher temperatures than the typical total oxidation tests with a NiO catalyst. Such temperatures are distributed in a narrow range, 250–350 °C, indicating the possible intervention of well-defined species. If we think of the above-mentioned role of adsorbed oxygen in NiO catalysis, it is tempting to hypothesize the role of similar species, possibly bonded to well-defined surface defects, in NiO sensing. It is a fascinating working hypothesis for further developments.
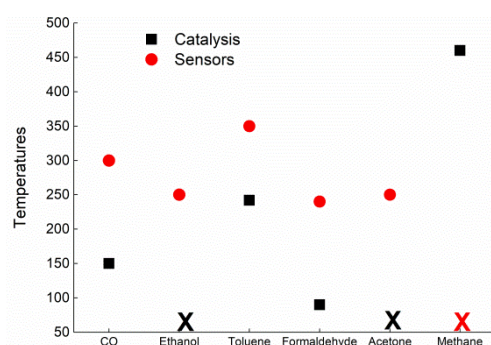
Figure 2. Best operating temperatures for the indicated sensing (best operating temperature and response tradeoff) and oxidation (lowest total combustion temperature) experiments over NiO materials. The crosses indicate the applications where no adequate references could be found. The references are reported in the discussion.

3.4. α-Cr₂O₃

The oxygen and CO chemisorption properties of α-Cr_2O_3 have been known for decades. In 1973, Yao reported the oxidation properties of unsupported chromia towards CO and various hydrocarbons (C_2H_4, C_3H_6, C_2H_6, and C_3H_8; all tests at 300 °C) [71]. Later on, mesoporous chromia was shown to be capable of eliminating 94% of toluene and 94% acetaldehyde at room temperature (1 g of catalyst was used in these tests) [72]. Another mesoporous chromia was successful in the total oxidation of ethyl acetate [73], while, later on, toluene (300 °C) and ethyl acetate (250 °C) total combustions were confirmed over

mesoporous chromia [74]. Low-temperature (200 °C) CO oxidation was more recently reported [75]. Finally, ethanol was considered, too, but it did not result in total oxidation (temperatures between 50 and 300 °C) [76].

On the contrary, gas-sensing studies of α-Cr_2O_3 are indeed few in number, despite spanning an interesting range of analytes. In 1994, Morrison and coworkers [77] tested α-Cr_2O_3 as a hydrogen sensor, which has not been further developed. Then, ethanol (200 ppm, 1.3 response at 250 °C) [78] and toluene (100 ppm, 170 °C, response 33.64) [79] sensing properties were reported by chromia nanotubes and porous microspheres, respectively. More recently, Ding et al. [80] reported sensing of 1 ppm formaldehyde at 230 °C, with a response of almost 25.

The sparse situation emerging from the literature review is reflected by the disordered appearance of the summary plot in Figure 3. It is difficult to discern clear trends, apart from the general use of high temperatures in total oxidation reactions, excluding the recent results for toluene and acetaldehyde. Surely, a remarkable input stems from testing several new analytes in gas-sensing, which is a positive result from reviewing chromia results. Another very important result is that one of the few papers published about chromia sensing contains fundamental clarifications about the possible issues of sensing by p-type materials [81]. In that paper, whose results were further developed by the same group [82], Pokhrel et al. concluded that while the reaction of ethanol with the material surface induced huge changes in terms of work function, such changes were not efficiently transduced in electrical signal modification. They argued that measuring resistance changes is not appropriate for p-type sensors. This fundamental observation must be recalled when dealing, in many cases, with very low responses from such materials. It could also explain why in many of the previous examples, all dealing with p-type semiconductors, a clear correlation between catalytic activity and sensor properties could not be firmly established.
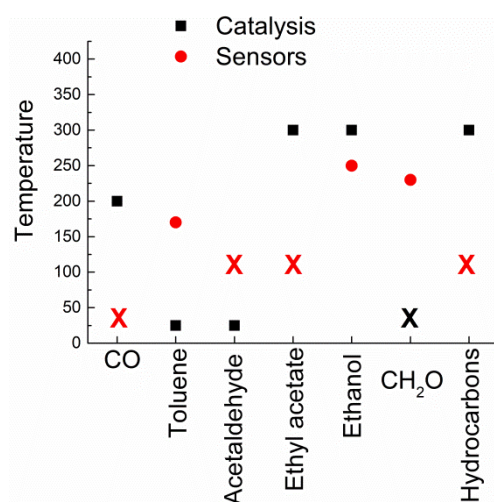
Figure 3. Best operating temperatures for the indicated sensing (best operating temperature and response tradeoff) and oxidation (lowest total combustion temperature) experiments over Cr_2O_3 materials. The crosses, not to be referred to any particular temperature, indicate the applications for which no adequate references could be found. The references are reported in the discussion.

3.5. Perovskites

The connection between oxide catalysis and oxide sensors is straightforward in the case of perovskites since oxygen vacancies are of paramount importance in determining the properties of perovskite materials [83], and their controlled generation is essential [84]. The vacancy concentration can control the oxygen adsorption behavior onto the perovskite surface [85], which is an essential feature both in catalytic and chemoresistive applications. This consideration holds for any other chemoresistive material, but perovskites have been under specific focus for a long time given their rich defect chemistry. The general perovskite

(perovskite itself is the name of the $CaTiO_3$ mineral, featuring a slightly distorted structure with respect to the ideal description given in the following) composition is described by the formula ABX_3, where X is an anion and A and B are metal cations, of which B is smaller than A and occupies X_6 octahedra, whereas the A cation is 12-fold coordinated [86]. For reaching +6 total oxidation state, there are multiple choices of A and B, which gives rise to a huge family of compounds [87,88] that is attracting more attention than ever [89] (constraints about the ion choice are related to the size ratio between anions and cations, as described by the Goldschmidt's rule [90]). Among such diverse properties, the catalytic ones have been of remarkable interest for a long time [87,88,91–96]. For instance, CO oxidation over $La_{0.65}Sr_{0.35}MnO_4$ was already reported in 1953 [97]. Because such properties have been studied for a long time, there are some established areas of knowledge, as summarized just below, that can be fruitful to workers in oxide sensors.

The ligand field approach to the understanding of the catalytic properties of perovskites has been stressed recently [92]. However, already in 1989, Tejuca et al. [95] could summarize several results about the role of the occupancy of the B 3d orbital in the $LaBO_3$ series, where La is a lanthanide (they recalled an early suggestion by Voorhoven [98], in turn referring to early work by Dowden [99]). It was shown that the CO oxidation activity increased when going (in terms of the occupancy of the 3d level of the B^{3+} cation) from vanadates to cobaltites, then decreasing again going from cobaltites to ferrites. Therefore, the influence of the B cation on the CO oxidation properties should be carefully taken into account when designing the composition of a CO and, possibly, of a generic VOC perovskite sensor [100]. Moreover, an investigation on the influence of the B cation could be a useful tool for gaining more insight into the sensing mechanisms of perovskites.

A further suggestion was the stoichiometry effect when keeping the B cation fixed and changing the A one in such a way to force different oxidation states of A, for instance, in the $CeCoO_3$ and $SrCoO_3$ couple, where Ce and Sr enhanced and decreased the CO oxidation activity, respectively ([95] and references therein).

The previous two points were considered as cornerstones in perovskite catalysis design by Misono [96]. He further suggested the exploitation of the synergistic effect of B-site elements. As an example, he reported the following scale of catalytic activities: $LaMn_{1-x}Cu_xO_3 >> LaMnO_3$, La_2CuO_4. These rules, accompanied by adequate knowledge of the catalytic applications of perovskites, could be helpful in designing gas sensors for given applications.

The attractive properties of perovskites have favored a remarkable proliferation of studies. It is difficult to find a unitary guideline: for instance, if one considers $LaFeO_3$, it gives rise to a whole family of compounds, depending on partial replacement of Fe by other cations, and it is possible to find catalytic applications for a given Fe content but sensing data for a slightly different Fe content. Therefore, we are going to propose a collection of indicative examples, using the gases as bullet points. A summary of the results is presented in Figure 4, where the scattered behavior of perovskites can be clearly observed.

As stated before, CO oxidation over perovskites is a very consolidated topic [48], and many materials have been tested. Nakamura et al. [101] studied a series of perovskites of general formula $La_{1-x}Sr_xCoO_3$, concluding that the increase in the Sr content favored CO oxidation, which was complete at 300 °C. Taguchi et al. [102] reported complete CO oxidation below 200 °C by $LaCoO_3$ prepared by a citrate method. The convenient oxidation conditions are in agreement with the predictions summarized in the review by Tejuca et al. [95] and Fierro [94], where the role of the electronic configuration of the B cation was evidenced. The powerful catalytic activity of cobaltites was also observed by Panich et al. [103], who investigated the catalytic activity of $M^IM^{II}O_3$ (M^I = La; M^{II} = Co, Mn, Cr, Al, Ni, and V) and M^ICoO_3 (M^I = Y, Nd, Sm, and Er) perovskites in the oxidation of CO and other species. $NdCoO_3$ resulted in total CO oxidation at 80 °C only. They also found that the rare earth element has no influence on the catalytic activity, in agreement with previous conclusions by Viswanathan [104]. Manganites, too, are known for their activity in CO oxidation [105]. Boroskikh et al. studied a series of $La_{1-x}Sr_xCoO_{3-\delta}$ (x = 0.0, 0.3, 0.5)

perovskites, finding that for x = 0.5 CO conversion to CO_2 was complete at 200 °C. A few papers have been published concerning CO sensing based on various lanthanum ferrites and cobaltites [106]. There is a remarkable agreement between the reported operating temperatures (250–270 °C for ferrites, 200–250 °C for cobaltites) and the expectable trends from the catalysis literature. However, moderate responses were obtained, ranging around unity or less, even for 50 or 100 ppm CO concentration [107,108], which places the problem of achieving efficient electronic transduction of the surface chemical reactions as typical with p-type semiconductors [63].
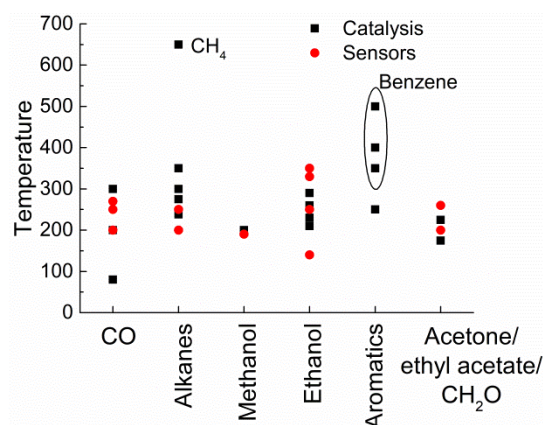
Figure 4. Best operating temperatures for the indicated sensing (best operating temperature and response tradeoff) and oxidation (lowest total combustion temperature) experiments over several perovskite materials. More points are present when an appreciable spread of the results was found. The references are reported in the discussion.

Many other applications of perovskites in total oxidation reactions are known [105]. As concerns alkanes, the total oxidation of methane is very critical for energy storage developments that a whole review has been devoted to the topic (a table with an extensive list of compositions is contained in that paper) [91]. However, temperatures larger than 600 °C were reported for the total combustion over $LaFeO_3$. On the other hand, Giang et al. [109] reported the detection of 200 ppm of methane, propane, and hexane, with a best operating temperature of about 200 °C and a corresponding response of 30%, 100% and 450%, respectively, reflecting the decreasing stability of the gases. The best performance was obtained with $NdFeO_3$ (methane) and $SmFeO_3$ (propane and hexane). Dhivya et al. reported a response of about 3.4% at 250 °C to 100 ppm methane by $CdTiO_3$. Ethane oxidation was observed between 300 and 400 °C over $La_{1-x}K_xMnO_{3+\delta}$ [110] and $SmCoO_3$ and $PrCoO_3$ [111]. Propane oxidation has been studied over several perovskites, for instance $La_{1-x}A'_xMnO_3$ (A' = Sr, Ce, Hf) [112], cobaltites ($La_{1-x}Ca_xCoO_3$) [113] and ferrites [114]. Its oxidation is easier than for ethane, with a light-off temperatures around 300 °C. Butane is even less stable, with light-off temperature of 275 °C over $LaMnO_3$ [115]. Finally, Szabo et al. [116] studied the *n*-hexane oxidation reaction of a series of $LaCo_{(1-x)}Fe_xO_3$ perovskites, finding complete conversion even at 238 °C. However, apartfrom the few examples quoted above, the sensing studies of alkanes heavier than methane are hard to find. These catalytic observations, instead, suggest that they could offer more convenient operating temperatures and larger responses than for methane. Moreover, the study of a series of alkanes, from the sensing point of view, could be enlightening about the mechanisms with the support of the existing catalysis literature.

Methanol combustion was studied over a series of $LaBO_3$ perovskites (B = Co, Mn, Fe) [117], and the authors found total conversion below 200 °C for $LaCoO_3$ and $LaMnO_3$. Ethanol combustion was studied, for instance, over $LaFe_{1-y}Ni_yO_3$ [118], with complete combustion just below 300 °C. Najjar and Batis found that $LaMnO_3$ prepared by the combustion method could completely oxidize ethanol at 210 °C [119]. Bialobok et al. pre-

pared [120] $LaCoO_3$, $La_{0.8}Sr_{0.2}CoO_3$, and $La_{0.95}Ce_{0.05}CoO_3$ by the combustion method and found that complete ethanol conversion to CO_2 occurred around 260 °C with small variations among the three materials. $La_{1-x}Ca_xMnO_3$. [121] could achieve the total conversion of ethanol below 230 °C. As a final example, $LaMnO_3$ could completely oxidize isopropanol to CO_2 at 240 °C [122]. Therefore, it can be seen that, by proper choice of the perovskite composition, the total oxidation temperature can be tuned for ethanol and methanol. Qin et al. [123] studied the methanol response to a series of perovskites of the general formula $La_{1-x}Mg_xFeO_3$, characterized by an ordered mesoporous structure. They found a maximum response (146.5) to 100 ppm methanol at 190 °C with the $La_{0.95}Mg_{0.05}FeO_3$ sensor. The low operating temperature is in agreement with the aforementioned low-temperature combustion of methanol over perovskites. Ethanol sensing by perovskites was investigated earlier by Obayashi et al. [124] in a very instructive paper. The authors studied the response to ethanol by a series of perovskites of general formula $LaBO_3$. They found that if B was Mn, there was no sensing activity, while for B = Fe, Co, and Ni, a response could be measured. For $LaNiO_3$, the sensing activity was greatly improved by partially substituting Fe for Ni, with a maximum response of about 300% at 350 °C for the compound $LaNi_{0.4}Fe_{0.6}O_3$. They also studied the $Ln_{0.5}Sr_{0.5}CoO_3$ (Ln: La, Pr, Sm, Gd) series, determining a huge response improvement (1200%, 330 °C, 150 ppm ethanol) when using Sm and substituting Co for Fe ($Sm_{0.5}Sr_{0.5}FeO_3$). Ge et al. [125] studied the ethanol-sensing properties of the $LaFe_{1-y}Co_yO_3$ series, determining, at 250 °C, a response of about 165 to a high ethanol concentration (1000 ppm) by the best-performing material in the series, $LaFe_{0.8}Co_{0.2}O_3$. In the $La_{1-x}Pb_xFeO_3$ series, Song et al. [126] found a maximum response (about 60) for x = 0.2 at an interesting temperature of 140 °C for, still, a rather high ethanol concentration (500 ppm). Cao et al. [127] prepared a series of $LaFe_xO_{3-\delta}$ perovskites, testing them as ethanol sensors. They found a convenient best operating temperature of 140 °C, with a maximum response to 1000 ppm of ethanol of about 125 for x = 0.8. The promising behavior of doped $LaFeO_3$ perovskites was further confirmed by Xiang et al. [128], who prepared a series of $La_{1-x}Ba_xFeO_3$ materials, establishing that, by using nanofibers of $La_{0.75}Ba_{0.25}FeO_3$, a response of 136.1 to 500 ppm of ethanol was obtained at 210 °C. Very recently, Hao et al. [129] reported a best operating temperature of 200 °C (response was about 180 for 200 ppm ethanol) for $La_{0.98}Ba_{0.02}FeO_3$ if compared with 260 °C of pure $LaFeO_3$.

　　　Perovskites have been used as catalysts for the oxidative decomposition of several other VOCs. For instance, benzene catalytic oxidation was studied by Einaga et al. [130] over $LaMO_3$ (M = Mn, Co, and Fe) and the series $La_{1-x}Sr_xMnO_3$. They found that 99% conversion was obtained for $LaMnO_3$ catalyst at 350 °C, whereas 500 °C was necessary for the 99% conversion with $LaCoO_3$ catalyst. In the Sr-doped series, 100% conversion was obtained at about 400 °C, depending on the calcination temperature of the materials, with the highest activity obtained for x = 0.6. Toluene was successfully oxidized over $La_{1-x}Sr_xMnO_{3-\delta}$ microcubes [131]. The authors obtained toluene complete oxidation at 255 °C with $La_{0.5}Sr_{0.5}MnO_{3-\delta}$ composition. Blasin-Aubé et al. [132] obtained a similar temperature for 99% toluene oxidation with $La_{0.8}Sr_{0.2}MnO_{3+x}$. $La_{1-x}Sr_xMO_{3-\delta}$ (M = Co, Mn; x = 0, 0.4), prepared by a citric acid route, showed 100% toluene conversion at about 220 °C for $La_{0.6}Sr_{0.4}CoO_{2.76}$ [133]. One of the lowest decomposition temperatures for ethyl acetate (175 °C) was obtained with $La_{0.6}Sr_{0.4}CoO_{2.78}$ [134]. Acetone total oxidation was studied over $LaMnO_3$ and $LaCoO_3$ [122], where $LaMnO_3$ (total oxidation to CO_2 at 225 °C) resulted in being more active than $LaCoO_3$. On the other hand, the detection of the just-mentioned analytes by perovskites presents very few examples (if we keep on focusing on noble metal-free materials). Xiao et al. [135] tested $LaFeO_3$ porous microspheres to 50 ppm acetone, obtaining a response of about 15 at 260 °C. Yao et al. [136] studied the formaldehyde sensing properties of $La_{1-x}Sr_xFeO_3$ perovskites prepared by sol–gel method and established that x = 0.3 provided the best sensing performance, with a response of 26 to 50 ppm formaldehyde at 200 °C.

In the reviews we have been quoting until now, the reader can find further references. Our aim here was to show that the perovskite catalysis provides specific, precious advice to chemoresistive sensing, pushing to always take into account the chemistry of defects and oxygen vacancies when trying to explain the sensing properties. In this sense, a notable example involving the full development of the defect chemistry of $SrTiO_3$ in the presence of La and Fe dopants was published in 1999 by Menesklou et al. [137]. The authors could conclude that 35% Fe-doping was effective in achieving temperature-independent oxygen sensors. The use of perovskites as oxygen sensors has been known for a long time, a whole review being devoted to the topic several years ago [106]. In the same paper, a summary was presented about the sensing of VOCs, such as methanol, ethanol, acetone, various alkanes, and ammonia, showing that even the interest for perovskites as VOCs sensors is not recent. More recently, other reviews have again stressed the ubiquitous application of perovskites in chemoresistive sensing [138,139]. Therefore, it is hoped that research on fundamental aspects may contribute solving such issues, such as the low response to many gases. Recent developments seem encouraging. For instance, the detection of H_2S by $LaFeO_3$ fibers prepared by electrospinning [140] was investigated. The authors could detect down to 0.5 ppm of SO_2 and H_2S with the best operating temperature at 250 °C. Both analytes behaved as reducing gases towards $LaFeO_3$, which is a p-type semiconductor, as most perovskites. The authors observed drift of the base conductance of the devices during SO_2 testing, which they attributed, by XPS investigation, to surface corrosion of the perovskite by SO_2 itself. Another noticeable example is the synthesis of $PbTiO_3$ nanoplatelets by Lee and coworkers [141]. The authors could detect 5 ppm of ethanol at 300 °C with a large response, thus allowing the detection of as low as 0.1 ppm ethanol concentration. The sensor signal was almost independent of the humidity in the environment.

A final remarkable example, further enlightening the effective connection between heterogeneous catalysis and chemoresistive perovskites, is offered by a paper published by the Tübingen group [142] concerning the sensing mechanisms of acetylene and ethylene over $LaFeO_3$. The authors employed DRIFT (diffuse reflectance infrared spectroscopy) and catalytic conversion measurements. They first established the interaction between CO_2 (which can be produced by hydrocarbons combustion and be re-adsorbed onto the sensor surface) and the sensor surface, and, on the basis of the results, the DRIFT spectra obtained during the exposure to ethylene and acetylene were interpreted. The remarkable result was that, for both gases, the mechanism at 150 °C proceeds through formate generation and a subsequent reaction with the surface oxygen species. The same did not hold at 250 °C for ethylene, which largely reacted with the platinum electrodes, resulting in the combustion and loss of sensor signal. It is the formate formation that results in conductance change (resistance increase), which is different from the usual mechanism of surface reduction/oxidation. The importance of this example lies in the advice to not systematically assume the usual hypotheses (oxygen chemisorption-surface regeneration) in analyzing the behavior of a gas sensor. Even the observation about the role of Pt electrodes is crucial and implicitly points to essential differences between chemoresistive sensors and heterogeneous catalysts.

3.6. α-Fe$_2$O$_3$

The alpha form of iron oxide, hematite, crystallizes in the corundum structure, similarly to α-Cr_2O_3, but presents n-type semiconductivity. The sensing applications of hematite span a huge range of particle morphologies, very often tested to acetone, ethanol and other VOCs [143]. Cuong et al. [144] reported one of the very few hematite CO sensors, with a response of 22.5 to 100 ppm CO at 300 °C. The data published in the literature for ethanol are remarkably uniform, with operating temperatures between 240–340 °C typically used to detect 100 ppm gas concentration and responses between 8 and 22, depending on the hematite morphology. In fact, the capabilities of controlling the shape of hematite nanoparticles are such that a review has been recently devoted to hematite

nanotubes only [145]. Recently, hematite hollow ellipsoids were prepared by a template method and tested for butanol sensing. It was found a decreased best operating temperature (217 °C) with respect to previous works for 100 ppm butanol [146]. Hollow nanoparticles were used for the detection of as low as 10 ppm acetone concentration at 200 °C and a response of about 6 [147]. Another interesting hematite morphology has been recently published, consisting of microcubes for high-temperature (400 °C) detection of ethanol (100 ppm). Hematite nano-ellipsoids were used to detect down to 5 ppm H_2S at 260 °C [148]. The comparison table presented by the authors, only concerning H_2S sensing by hematite, is sufficient to testify about the flourishing sensing research on hematite sensors. A remarkable spread of operating conditions could be observed, with operating temperatures ranging from 50 to 350 °C, gas concentrations from 0.05 to 100 ppm, but responses comprised in a very narrow range, from 2.58 (Fe_2O_3 nanoboxes [149], 50 °C, 5 ppm concentration) to 11.7 (Fe_2O_3 micro-ellipsoids [150], 350 °C 100 ppm concentration). Surely, morphology plays a role in this peculiar set of results, but it is confirmed the difficulty in finding suitable interpretation frames for gas sensors.

Despite hematite has been used throughout the years as a catalyst for the oxidation of CO [151–153] (temperatures ranging from 225 to 350 °C) and the total oxidation of various VOCs such as methane [154] (high operating temperatures between 600 and 700 °C), propane [155,156] (complete combustion at 400 °C), and toluene [156] (complete combustion at 250 °C), only some of these analytes have been tested by hematite sensors. There are few or no studies concerning methane and propane, which could be investigated by taking advantage of the high-temperature stability of hematite.

The limited interaction that has been emerging between hematite catalysts and sensors is apparent in Figure 5, where some of the most interesting operating temperatures have been reported for various gases. It is not even necessary to mark missing applications, as done in previous figures, since it was only possible to find results for CO in the two fields. However, the interesting low-temperature total oxidation of toluene could be attractive, for instance, to develop a hematite sensor for such gas. Therefore, it seems worth considering more in detail the possible sensing of these gases by hematite, also taking advantage of the thermal stability of the material up to high temperatures. Moreover, there is no definite attempt of finding a clear connection between the sensing properties and the catalytic activity of hematite. Such investigation is desirable since the investigation of the surface chemistry of iron oxides is at an advanced stage [157].
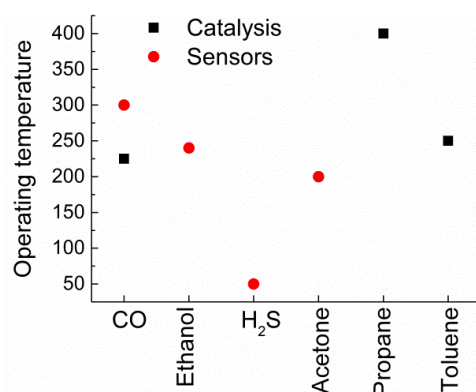
Figure 5. Typical operating temperatures for the indicated sensing and catalytic experiments with Fe_2O_3 materials, as found in the literature. The crosses indicate the applications where no adequate references could be found. The references are reported in the discussion.

3.7. Semiconducting Oxide-Supported Catalysts

From the first section, we have slowly been shifting from p-type semiconductors, despite showing some notable exceptions depending on the composition and temperatures (perovskites) to an insulator, such as hematite, featuring however n-type conductivity in ordinary conditions. We can now finally enter the field of n-type semiconductors. Here we

refer to those catalysts which, differently from catalysts supported onto insulating alumina, silica etc., are based on semiconducting supports such as TiO_2 and SnO_2. The notable finding is that the n-type semiconductivity of the pure support is preserved even after depositing the catalyst, allowing the study of such materials as chemoresistive sensors. One could argue that even catalysts supported on p-type supports are not unusual. The important difference is that in the class of materials that we are going to consider, there are no discrete particles of noble metals or of another oxide deposited onto the support. Instead, a monolayer of active oxide is deposited onto the support [158,159], originating an important synergistic effect.

3.7.1. V_2O_5-TiO_2 and SnO_2-V_2O_5

Such is the case of one the most popular and versatile catalysts in this class, TiO_2-supported V_2O_5. After a perusal of the extensive literature about TiO_2-V_2O_5, one could wonder why we decided to test it as a gas sensor. Indeed, if we accept that the sensing material must promote total combustion of the analyte, we see that TiO_2-V_2O_5 is well known for the total oxidation of chlorobenzenes [160–162] and showed moderate activity toward benzene total oxidation [163]. Even though the detection of such compounds is surely of interest, it could still be a very niche application. On the other hand, TiO_2-V_2O_5 is able of catalyzing the oxidation of many organic substrates to other useful compounds, as summarized regularly in the past [159,164–166]. Notable reactions include early work on oxidation of o-xylene to phtalic anhydride [167] and partial oxidation of methanol to formaldehyde [168]; oxidative dehydrogenation of propane [169]; ammoxidation reactions [170,171], etc. While the interested reader is referred to the quoted reviews for further details about supported V_2O_5, here, we face a question directly related to the development of chemoresistive sensors, i.e., in which way the just-mentioned reactions can result in attractive sensing properties since they could, at most, convert an analyte into another? The answer is the guess that such versatile catalysts as supported vanadia may convert the original analyte into other, more active species. We have seen a clear, recent example related to perovskites before [142]: the conversion of acetylene to formate resulted in enhanced sensing by the effect of the formate itself. Summarizing: supported vanadia invites going beyond the view of the total oxidation of the analyte during the sensing operation. However, such systems were scarcely studied as sensors, which was an additional stimulus to the development of sensing applications. In 2013, a paper was published [172] where a colloidal version of the $TiO_2@V_2O_5$ system was prepared by solvothermal synthesis, characterized by: stability against phase segregation up to 400 °C; limited grain growth upon heat-treatment (<5 nm); surface deposition of V_2O_5 layers onto the TiO_2 core material. The materials were tested for ethanol sensing, taken as a typical VOC example. The $TiO_2@V_2O_5$ displayed a response two orders of magnitude larger than pure TiO_2 toward 100 ppm of ethanol at 200 °C, with an estimated detection limit below 10 ppm. In the following work [173], it was interestingly shown that for both ethanol and acetone, the response was activated at much lower temperatures for $TiO_2@V_2O_5$ than for TiO_2. Then, the response decreased at higher temperatures, while for pure TiO_2, it hardly increased. Such a low-temperature operation seemed clearly attributable to catalytic activation of different reaction pathways by $TiO_2@V_2O_5$. This result confirmed the strength of the initial, catalysis-based concept and pushed to the developments of other systems, which are now going to discuss briefly.

Some more consideration can be added concerning the catalytic properties SnO_2-V_2O_5, which were observed very early [174], concerning oxidation of 1-butene and 1,3 butadiene and the dehydration and dehydrogenation of isopropyl alcohol. Then, the oxidation of propylene, ethylene, propane and CO was investigated [175]. Throughout the years, several other reactions have been investigated: for instance, ethane oxidative dehydrogenation [176], oxidation of o-xylene [177] and 2-propanol [178], Beckmann rearrangement of cyclohexanone oxime to ε-caprolactam [179]. Analogously to TiO_2-V_2O_5, such varied

catalytic activity seems attractive for potential gas-sensing properties, despite SnO_2-V_2O_5, overall, does not result as a very popular catalyst.

To the best of our knowledge, there are very few papers concerning SnO_2/TiO_2 supports and V_2O_5 [180–182]. Interestingly, in ref. [182] the authors studied the catalytic and sensing activity of V-SnO_2 nanoparticles (V_2O_5-SnO_2 solid solutions), despite they observed only slight NO_2 sensing enhancement by V addition to SnO_2. Zhang et al. [180] also explicitly relied on the catalytic properties of V_2O_5 for successfully making SnO_2 selective to specific VOCs (benzene, toluene, ethylbenzene, and xylene). The path is then fully open for further sensing applications of supported oxide systems.

3.7.2. Miscellanea of Other Semiconducting Oxide-Supported Catalysts

It is now immediate to conceive new systems, simply looking at the catalogue of supported catalysts and relying on appropriate synthetic chemistry. We will shortly discuss two more examples and propose one more system for NO_x detection. Keeping the same TiO_2 support, two other related heterogeneous catalysts are well-known: TiO_2-WO_x and TiO_2-MoO_x, where the *x* subscript describes the variable oxidation state of the surface oxide.

TiO_2-WO_x has been employed in a much more limited range of reactions than TiO_2-V_2O_5, such as alkene isomerization [183], selective oxidation of cyclopentene [184], conversion of glycerol to acrolein [185] and, interestingly, isopropanol dehydration [186]. The interesting conversion properties of several different organic substrates pushed to the preparation of a TiO_2-WO_x gas sensor [187]. A colloidal synthesis was developed, analogous to that employed for TiO_2-V_2O_5 [172], with nominal atomic concentrations of W to Ti ranging from 16% to 64%. Upon heat-treatment to 500 °C, WO_3-surface coated TiO_2 anatase nanocrystals were obtained for 16% W concentration or a nanocomposite where WO_3 nanocrystals were mixed with the surface modified titania host, for 64% W concentration. Ethanol was chosen as prototypal gas amenable to oxidation reactions. The sensing tests showed surprising response enhancement. Not depending on the starting W concentration, the response was magnified by two orders of magnitude with respect to pure TiO_2 at a temperature of only 200 °C. Pure TiO_2 displayed opposite behavior, just as described above for TiO_2-V_2O_5, needing much higher operating temperatures for reaching a however limited response. A potential detection limit below 10 ppm ethanol concentration was evident. In the following work [188], the acetone sensing properties were investigated. Here a response enhancement by three orders of magnitude with respect to pure TiO_2 was measured. Both in acetone and ethanol, a simple surface layer of WO_3 was therefore sufficient to provide the TiO_2 core by response properties similar to pure WO_3, which by itself is a powerful acetone sensor [189]. To the best of our knowledge, the few works devoted to gas-sensing by TiO_2-WO_3 present nanocomposite materials typology, where WO_3 and TiO_2 discrete nanoparticles exist. Instead, the just discussed work further pushes to developing catalysis-related systems. This consideration was pushed to the last system we are going to review.

TiO_2-supported MoO_x is well known for selective oxidation of methanol to formaldehyde [190–194] and of ethanol to mainly formaldehyde [195], but it has also been used for dehydrosulfurization reactions [196] and ammoxidation of 3-picoline [197]. A colloidal version of the TiO_2-MoO_x system was once again prepared by the techniques that were used for TiO_2-V_2O_5 and TiO_2-WO_3 [198]. The various nominal atomic concentration of Mo with respect to Ti were considered, ranging from 23% to 92%. Only for the lowest Mo concentration, the desired surface modification of TiO_2 by MoO_3 was obtained after heat-treatment at 500 °C. Larger concentrations resulted in phase segregation of Mo oxides. Once again, a remarkable enhancement of the sensing properties was observed with respect to pure TiO_2, for all the considered Mo concentrations, in particular, as concerns acetone sensing. A response increase by two orders of magnitude was observed at 300 °C, with a calculated detection limit of 1 ppm. Comparable enhancement was also observed for CO, a gas to which pure TiO_2 is typically very poorly responsive.

Other interesting catalysts can be suggested, such as those for NO removal, which partly belong to the already discussed typologies but also include new materials such as V_2O_5-MoO_3/TiO_2 [199]. Instead, we hope that the present, short view over heterogeneous catalysts may be clarifying towards the beneficial contribution that can be given to the gas-sensing field.

4. Reactions and Mechanisms

All the oxide catalysts described until now have been considered for their activity in combustion reactions, i.e., the total conversion of the gas to CO_2. It is not excluded that they can be used as catalysts for partial oxidation (e.g., alcohol to aldehyde), but it is combustion that is of main interest for chemical sensing (in Section 3.7, we have seen that conversion to other analytes was the base for the development of specific sensors). The reason is the generally accepted principle of operation of chemoresistive oxide sensors (for reducing gases) [200]:
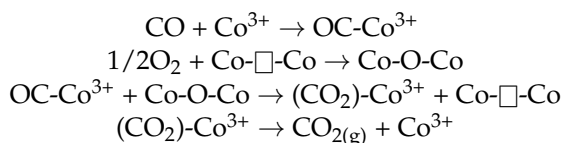
(i)   oxygen adsorption onto the sensor surface, implying charge extraction from the sensing material itself;

(ii) reaction of the analyte with the sensor surface, implying consumption of surface oxygen, and restoring charge into the semiconducting sensing material.

The step implying "consumption of surface oxygen" is generally represented as a combustion reaction. Therefore, an exchange between metal oxide catalysis and sensing seems natural. However, the representation of the surface–gas interaction through a combustion reaction is only a schematic one, summarizing the overall outcome of the various steps involved in the reaction. Even the combustion of CO is only schematically represented by the equation:

$$CO + 1/2\,O_2 \rightarrow CO_2$$

Actually, a Mars–van Krevelen mechanism [201,202] generally operates onto metal oxide surfaces, implying several steps, even for CO, as we shall see below. This consideration leads to a remarkable discrepancy between the state of the art of catalysts and that of sensors. The knowledge of the mechanisms is very much detailed for several oxide catalyzed reactions. Such science is still in its infancy in the case of sensors. We have been referring in the previous discussion to some of the very few known examples. More work has been carried out in the case of SnO_2 sensors [6,203] with noble metal additives. However, overall, the knowledge of mechanisms in gas sensors is very far from being comparable with catalysis. There are some specific reasons for this situation. First of all, dealing with electrically connected devices introduces remarkable technical limitations with respect to the typical catalysis setup. Secondly, the amount of gas reacting with the sensor surface is much less with respect to the catalytic reactions seen above, where it can reach a few % in volume, to be compared with the few ppm of gas-sensing. The consequence is that the analysis of the evolved species from a gas sensor suffers from remarkable noise with respect to catalysis. An additional problem is that a gas sensor will necessarily work in a humid atmosphere. Therefore, studying a mechanism in a dry atmosphere is surely useful but not as a representative of the real sensor operation as the mechanism in the presence of humidity. The problem is that water vapor is a powerful interference and severely complicates the study of the mechanism. A further problem can be, as observed, for instance in [142], that the electrodes of the sensor may constitute a remarkable perturbation of the sensing process. Finally, a huge issue is that, in the case of chemosensors, understanding the mechanism additionally means that it is necessary to provide a model for the electrical properties modification due to the surface reactions. It is necessary to further add that it is not straightforward to transfer the catalysis mechanisms to the same materials used as gas sensors. One reason is that the gas concentrations used in catalysis result in surface coverage of the catalyst much different from gas sensors, with a consequent possible switch to other mechanisms. We can see another reason by a simple

example. In the case of CO oxidation over Co_3O_4, it is largely accepted that the reaction proceeds through a Mars–van Krevelen mechanism [48]:

$$CO + Co^{3+} \rightarrow OC\text{-}Co^{3+}$$
$$1/2O_2 + Co\text{-}\square\text{-}Co \rightarrow Co\text{-}O\text{-}Co$$
$$OC\text{-}Co^{3+} + Co\text{-}O\text{-}Co \rightarrow (CO_2)\text{-}Co^{3+} + Co\text{-}\square\text{-}Co$$
$$(CO_2)\text{-}Co^{3+} \rightarrow CO_{2(g)} + Co^{3+}$$

where the $\square$ symbol indicates an oxygen vacancy. In ref. [19], as described above in Section 3.1, the authors found opposite behavior to CO by Co_3O_4 sensor with respect to catalytic conversion, which increased at high temperatures while the sensor response decreased. The Mars–van Krevelen mechanism, by itself, does not provide any specific hint. However, it is still debated which vacancies are involved in the catalytic process. Therefore, it can be guessed that different surface sites are involved in the sensing process with respect to catalysis and that the latter are not contributing to the electrical process.

It is very often encountered in gas-sensing papers, a section devoted to sensing mechanisms. Typically, the above-mentioned modulation of the charge density in the sensing material (modulation of the depletion layer) is invoked due to a reaction that is always reported as combustion. However, it must be kept in mind that this kind of approach only replicates the steps given in points (i) and (ii) above, but no insight is gained until the hypothesis of combustion is properly supported and until it is not recognized that the combustion reaction can only represent the overall reaction. Knowledge of the mechanisms requires elucidating its steps with the just-mentioned additional difficulties with respect to catalysis. Many techniques have been fully developed for studying the catalytic reactions, but only in a few cases, it is possible to find the measurement of the catalytic conversion properties [19] and the use of isotopic labeling [203], as conducted by the Tübingen group and in papers by Yamazoe and coworkers. Additionally, DRIFT spectroscopy, to the best of our knowledge, is mainly being used by the same group, as concerns the gas-sensing field.

5. Conclusions

Several reasons of interest for metal oxide catalysis, as observed from the chemosensors field, appear. Several potential applications and "advice" have been highlighted for metal oxide gas sensors:

1. Metal oxide heterogeneous catalysts such as Co_3O_4, CuO and perovskites seem to have already been profitably exploited as chemoresistive sensors. However, several analytes such as alkanes and aromatics still deserve further attention.
2. Other catalysts deserve more attention, such as α-Cr_2O_3 and manganese oxides.
3. The field of supported (onto semiconducting oxides) catalysts seems very promising, and it deserves further investigation. It is only limited by the synthetic ability in preparing any novel material available by coupling single oxides: SnO_2-MoO_3, SnO_2-WO_3, TiO_2-Fe_2O_3, etc.
4. The design rule for perovskite catalysts is of potential interest for the design of chemosensors too.
5. The presence and nature of oxygen vacancies deserve particular attention. This means that they must be carefully identified, characterized, and related to the ongoing reactions. This achievement only can provide further insight into the connections between heterogeneous catalysis and chemoresistive sensors.

    However:

6. The connection between catalysts and their applications as gas sensors is not straightforward. It may happen that a good catalyst for a given gaseous reaction does not provide an outstanding sensing response to the same gas, or vice versa. Recent findings suggest that, indeed, different species and/or mechanisms may be involved in the two application fields. This is just one stimulus more to deepen the knowledge of

the sensing mechanisms, which can only beneficially draw from the well-established field of catalysis mechanisms.

We, however, hope that the discussion illustrated in the present work can just be a stimulus to face these fascinating questions.

References

1. Müller, S.A.; Degler, D.; Feldmann, C.; Türk, M.; Moos, R.; Fink, K.; Studt, F.; Gerthsen, D.; Bârsan, N.; Grunwaldt, J.-D. Exploiting Synergies in Catalysis and Gas Sensing using Noble Metal-Loaded Oxide Composites. *ChemCatChem* **2018**, *10*, 864–880. [CrossRef]
2. Xiong, M.; Gao, Z.; Qin, Y. Spillover in Heterogeneous Catalysis: New Insights and Opportunities. *ACS Catal.* **2021**, *11*, 3159–3172. [CrossRef]
3. Conner, W.C.; Falconer, J.L. Spillover in Heterogeneous Catalysis. *Chem. Rev.* **1995**, *95*, 759–788. [CrossRef]
4. Yamazoe, N.; Kurokawa, Y.; Seiyama, T. Effects of additives on semiconductor gas sensors. *Sens. Actuators B* **1983**, *4*, 283–289. [CrossRef]
5. Neri, G. First Fifty Years of Chemoresistive Gas Sensors. *Chemosensors* **2015**, *3*, 1–20. [CrossRef]
6. Degler, D.; Müller, S.A.; Doronkin, D.E.; Wang, D.; Grunwaldt, J.-D.; Weimar, U.; Barsan, N. Platinum loaded tin dioxide: A model system for unravelling the interplay between heterogeneous catalysis and gas sensing. *J. Mater. Chem. A* **2018**, *6*, 2034–2046. [CrossRef]
7. Degler, D.; Weimar, U.; Barsan, N. Current Understanding of the Fundamental Mechanisms of Doped and Loaded Semiconducting Metal-Oxide-Based Gas Sensing Materials. *ACS Sens.* **2019**, *4*, 2228–2249. [CrossRef] [PubMed]
8. Williams, D.E.; Henshaw, G.S.; Pratt, K.F.E.; Peat, R. Reaction–diffusion effects and systematic design of gas-sensitive resistors based on semiconducting oxides. *J. Chem. Soc. Faraday Trans.* **1995**, *91*, 4299–4307. [CrossRef]
9. Védrine, J.C. Importance, features and uses of metal oxide catalysts in heterogeneous catalysis. *Chin. J. Catal.* **2019**, *40*, 1627–1636. [CrossRef]
10. Védrine, J.C. Metal Oxides in Heterogeneous Oxidation Catalysis: State of the Art and Challenges for a More Sustainable World. *ChemSusChem* **2019**, *12*, 577–588. [CrossRef]
11. Bion, N.; Can, F.; Courtois, X.; Duprez, D. Transition metal oxides for combustion and depollution processes. In *Metal Oxides in Heterogeneous Catalysis*; Védrine, J.C., Ed.; Elsevier: Amsterdam, The Netherlands, 2018; pp. 287–353. [CrossRef]
12. Xu, H.; Yan, N.; Qu, Z.; Liu, W.; Mei, J.; Huang, W.; Zhao, S. Gaseous Heterogeneous Catalytic Reactions over Mn-Based Oxides for Environmental Applications: A Critical Review. *Environ. Sci. Technol.* **2017**, *51*, 8879–8892. [CrossRef]
13. Védrine, J.C. Heterogeneous Catalysis on Metal Oxides. *Catalysts* **2017**, *7*, 341. [CrossRef]
14. Malik, R.; Tomer, V.K.; Mishra, Y.K.; Lin, L. Functional gas sensing nanomaterials: A panoramic view. *Appl. Phys. Rev.* **2020**, *7*, 021301. [CrossRef]
15. Jeong, S.-Y.; Kim, J.-S.; Lee, J.-H. Rational Design of Semiconductor-Based Chemiresistors and their Libraries for Next-Generation Artificial Olfaction. *Adv. Mater.* **2020**, *32*, 2002075. [CrossRef]
16. Xu, J.M.; Cheng, J.P. The advances of Co_3O_4 as gas sensing materials: A review. *J. Alloy. Compd.* **2016**, *686*, 753–768. [CrossRef]
17. Cunningham, D.A.H.; Kobayashi, T.; Kamijo, N.; Haruta, M. Influence of dry operating conditions: Observation of oscillations and low temperature CO oxidation over Co_3O_4 and Au/Co_3O_4 catalysts. *Catal. Lett.* **1994**, *25*, 257–264. [CrossRef]
18. Xie, X.; Li, Y.; Liu, Z.-Q.; Haruta, M.; Shen, W. Low-temperature oxidation of CO catalysed by Co_3O_4 nanorods. *Nature* **2009**, *458*, 746–749. [CrossRef] [PubMed]

19. Wicker, S.; Großmann, K.; Bârsan, N.; Weimar, U. Co$_3$O$_4$—A systematic investigation of catalytic and gas sensing performance under variation of temperature, humidity, test gas and test gas concentration. *Sens. Actuators B Chem.* **2013**, *185*, 644–650. [CrossRef]

20. Deng, J.; Wang, L.; Lou, Z.; Zhang, T. Fast response/recovery performance of comb-like Co$_3$O$_4$ nanostructure. *RSC Adv.* **2014**, *4*, 21115–21120. [CrossRef]

21. Dissanayake, S.; Wasalathanthri, N.; Amin, A.S.; He, J.; Poges, S.; Rathnayake, D.; Suib, S.L. Mesoporous Co$_3$O$_4$ catalysts for VOC elimination: Oxidation of 2-propanol. *Appl. Catal. A Gen.* **2020**, *590*, 117366. [CrossRef]

22. Fedorov, F.S.; Solomatin, M.A.; Uhlemann, M.; Oswald, S.; Kolosov, D.A.; Morozov, A.; Varezhnikov, A.S.; Ivanov, M.A.; Grebenko, A.K.; Sommer, M.; et al. Quasi-2D Co$_3$O$_4$ nanoflakes as an efficient gas sensor versus alcohol VOCs. *J. Mater. Chem. A* **2020**, *8*, 7214–7228. [CrossRef]

23. Choi, K.-I.; Kim, H.-R.; Kim, K.-M.; Liu, D.; Cao, G.; Lee, J.-H. C$_2$H$_5$OH sensing characteristics of various Co$_3$O$_4$ nanostructures prepared by solvothermal reaction. *Sens. Actuators B Chem.* **2010**, *146*, 183–189. [CrossRef]

24. Marcoccia, C.G.; Peluso, M.A.; Sambeth, J.E. Synthesis, characterization and catalytic properties of cobalt oxide recovered from spent lithium-ion batteries. *Mol. Catal.* **2020**, *481*, 110223. [CrossRef]

25. Lü, Y.; Zhan, W.; He, Y.; Wang, Y.; Kong, X.; Kuang, Q.; Xie, Z.; Zheng, L. MOF-Templated Synthesis of Porous Co$_3$O$_4$ Concave Nanocubes with High Specific Surface Area and Their Gas Sensing Properties. *ACS Appl. Mater. Interfaces* **2014**, *6*, 4186–4195. [CrossRef] [PubMed]

26. Tang, W.; Xiao, W.; Wang, S.; Ren, Z.; Ding, J.; Gao, P.-X. Boosting catalytic propane oxidation over PGM-free Co$_3$O$_4$ nanocrystal aggregates through chemical leaching: A comparative study with Pt and Pd based catalysts. *Appl. Catal. B Environ.* **2018**, *226*, 585–595. [CrossRef]

27. Hu, L.; Peng, Q.; Li, Y. Selective Synthesis of Co$_3$O$_4$ Nanocrystal with Different Shape and Crystal Plane Effect on Catalytic Property for Methane Combustion. *J. Am. Chem. Soc.* **2008**, *130*, 16136–16137. [CrossRef]

28. Epifani, M.; Tang, P.-Y.; Genç, A.; Morante, J.R.; Arbiol, J.; Díaz, R.; Wicker, S. The Ethylhexanoate Route to Metal Oxide Nanocrystals: Synthesis of CoO Nanooctahedra from Co(II) 2-Ethylhexanoate. *Eur. J. Inorg. Chem.* **2016**, *2016*, 3963–3968. [CrossRef]

29. Wang, Z.; Wang, W.; Zhang, L.; Jiang, D. Surface oxygen vacancies on Co$_3$O$_4$ mediated catalytic formaldehyde oxidation at room temperature. *Catal. Sci. Technol.* **2016**, *6*, 3845–3853. [CrossRef]

30. Kim, J.Y.; Choi, N.-J.; Park, H.J.; Kim, J.; Lee, D.-S.; Song, H. A Hollow Assembly and Its Three-Dimensional Network Formation of Single-Crystalline Co$_3$O$_4$ Nanoparticles for Ultrasensitive Formaldehyde Gas Sensors. *J. Phys. Chem. C* **2014**, *118*, 25994–26002. [CrossRef]

31. Zhang, W.; Díez-Ramírez, J.; Anguita, P.; Descorme, C.; Valverde, J.L.; Giroir-Fendler, A. Nanocrystalline Co$_3$O$_4$ catalysts for toluene and propane oxidation: Effect of the precipitation agent. *Appl. Catal. B Environ.* **2020**, *273*, 118894. [CrossRef]

32. Deng, J.; Zhang, R.; Wang, L.; Lou, Z.; Zhang, T. Enhanced sensing performance of the Co$_3$O$_4$ hierarchical nanorods to NH$_3$ gas. *Sens. Actuators B Chem.* **2015**, *209*, 449–455. [CrossRef]

33. Petryk, J.; Kołakowska, E. Cobalt oxide catalysts for ammonia oxidation activated with cerium and lanthanum. *Appl. Catal. B Environ.* **2000**, *24*, 121–128. [CrossRef]

34. Post, J.E. Manganese oxide minerals: Crystal structures and economic and environmental significance. *Proc. Natl. Acad. Sci. USA* **1999**, *96*, 3447–3454. [CrossRef]

35. Chabre, Y.; Pannetier, J. Structural and electrochemical properties of the proton/γ-MnO$_2$ system. *Prog. Solid State Chem.* **1995**, *23*, 1–130. [CrossRef]

36. Albering, J.H. Structural Chemistry of Manganese Dioxide and Related Compounds. In *Handbook of Battery Materials*; Daniel, C., Besenhard, J.O., Eds.; Wiley-VCH: Weinheim, Germany, 2011; pp. 87–123. [CrossRef]

37. Kim, S.C.; Shim, W.G. Catalytic combustion of VOCs over a series of manganese oxide catalysts. *Appl. Catal. B Environ.* **2010**, *98*, 180–185. [CrossRef]

38. Lamaita, L.; Peluso, M.A.; Sambeth, J.E.; Thomas, H.J. Synthesis and characterization of manganese oxides employed in VOCs abatement. *Appl. Catal. B Environ.* **2005**, *61*, 114–119. [CrossRef]

39. Miao, L.; Wang, J.; Zhang, P. Review on manganese dioxide for catalytic oxidation of airborne formaldehyde. *Appl. Surf. Sci.* **2019**, *466*, 441–453. [CrossRef]

40. Zhu, S.; Wang, J.; Nie, L. Progress of Catalytic Oxidation of Formaldehyde over Manganese Oxides. *ChemistrySelect* **2019**, *4*, 12085–12098. [CrossRef]

41. Li, J.; Li, L.; Cheng, W.; Wu, F.; Lu, X.; Li, Z. Controlled synthesis of diverse manganese oxide-based catalysts for complete oxidation of toluene and carbon monoxide. *Chem. Eng. J.* **2014**, *244*, 59–67. [CrossRef]

42. Bigiani, L.; Zappa, D.; Maccato, C.; Gasparotto, A.; Sada, C.; Comini, E.; Barreca, D. Hydrogen Gas Sensing Performances of p-Type Mn$_3$O$_4$ Nanosystems: The Role of Built-in Mn$_3$O$_4$/Ag and Mn$_3$O$_4$/SnO$_2$ Junctions. *Nanomaterials* **2020**, *10*, 511. [CrossRef]

43. Bigiani, L.; Maccato, C.; Carraro, G.; Gasparotto, A.; Sada, C.; Comini, E.; Barreca, D. Tailoring Vapor-Phase Fabrication of Mn$_3$O$_4$ Nanosystems: From Synthesis to Gas-Sensing Applications. *ACS Appl. Nano Mater.* **2018**, *1*, 2962–2970. [CrossRef]

44. Na, C.W.; Park, S.-Y.; Chung, J.-H.; Lee, J.-H. Transformation of ZnO Nanobelts into Single-Crystalline Mn$_3$O$_4$ Nanowires. *ACS Appl. Mater. Interfaces* **2012**, *4*, 6565–6572. [CrossRef]

45. Tian, X.; Yang, L.; Qing, X.; Yu, K.; Wang, X. Trace level detection of hydrogen gas using birnessite-type manganese oxide. *Sens. Actuators B Chem.* **2015**, *207*, 34–42. [CrossRef]

46. Stobbe, E.R.; de Boer, B.A.; Geus, J.W. The reduction and oxidation behaviour of manganese oxides. *Catal. Today* **1999**, *47*, 161–167. [CrossRef]

47. Gawande, M.B.; Goswami, A.; Felpin, F.-X.; Asefa, T.; Huang, X.; Silva, R.; Zou, X.; Zboril, R.; Varma, R.S. Cu and Cu-Based Nanoparticles: Synthesis and Applications in Catalysis. *Chem. Rev.* **2016**, *116*, 3722–3811. [CrossRef]

48. Royer, S.; Duprez, D. Catalytic Oxidation of Carbon Monoxide over Transition Metal Oxides. *ChemCatChem* **2011**, *3*, 24–65. [CrossRef]

49. Zedan, A.F.; Mohamed, A.T.; El-Shall, M.S.; AlQaradawi, S.Y.; AlJaber, A.S. Tailoring the reducibility and catalytic activity of CuO nanoparticles for low temperature CO oxidation. *RSC Adv.* **2018**, *8*, 19499–19511. [CrossRef]

50. Steinhauer, S. Gas Sensors Based on Copper Oxide Nanomaterials: A Review. *Chemosensors* **2021**, *9*, 51. [CrossRef]

51. Rydosz, A. The Use of Copper Oxide Thin Films in Gas-Sensing Applications. *Coatings* **2018**, *8*, 425. [CrossRef]

52. Wang, L.; Zhang, R.; Zhou, T.; Lou, Z.; Deng, J.; Zhang, T. Concave Cu_2O octahedral nanoparticles as an advanced sensing material for benzene (C_6H_6) and nitrogen dioxide (NO_2) detection. *Sens. Actuators B Chem.* **2016**, *223*, 311–317. [CrossRef]

53. Park, H.J.; Choi, N.-J.; Kang, H.; Jung, M.Y.; Park, J.W.; Park, K.H.; Lee, D.-S. A ppb-level formaldehyde gas sensor based on CuO nanocubes prepared using a polyol process. *Sens. Actuators B Chem.* **2014**, *203*, 282–288. [CrossRef]

54. Steinhauer, S.; Chapelle, A.; Menini, P.; Sowwan, M. Local CuO Nanowire Growth on Microhotplates: In Situ Electrical Measurements and Gas Sensing Application. *ACS Sens.* **2016**, *1*, 503–507. [CrossRef]

55. Wang, F.; Li, H.; Yuan, Z.; Sun, Y.; Chang, F.; Deng, H.; Xie, L.; Li, H. A highly sensitive gas sensor based on CuO nanoparticles synthetized via a sol–gel method. *RSC Adv.* **2016**, *6*, 79343–79349. [CrossRef]

56. Li, D.; Tang, Y.; Ao, D.; Xiang, X.; Wang, S.; Zu, X. Ultra-highly sensitive and selective H_2S gas sensor based on CuO with sub-ppb detection limit. *Int. J. Hydrogen Energy* **2019**, *44*, 3985–3992. [CrossRef]

57. Parravano, G. The Catalytic Oxidation of Carbon Monoxide on Nickel Oxide. I. Pure Nickel Oxide. *J. Am. Chem. Soc.* **1953**, *75*, 1448–1451. [CrossRef]

58. Wang, F.; Xu, Y.; Liu, X.; Liu, Y.; Liu, J.; Teng, B. Pinpointing the active sites and reaction mechanism of CO oxidation on NiO. *Phys. Chem. Chem. Phys.* **2019**, *21*, 17852–17858. [CrossRef]

59. Wang, H.; Guo, W.; Jiang, Z.; Yang, R.; Jiang, Z.; Pan, Y.; Shangguan, W. New insight into the enhanced activity of ordered mesoporous nickel oxide in formaldehyde catalytic oxidation reactions. *J. Catal.* **2018**, *361*, 370–383. [CrossRef]

60. Xia, Y.; Lin, M.; Ren, D.; Li, Y.; Hu, F.; Chen, W. Preparation of high surface area mesoporous nickel oxides and catalytic oxidation of toluene and formaldehyde. *J. Porous Mater.* **2017**, *24*, 621–629. [CrossRef]

61. Bai, G.; Dai, H.; Deng, J.; Liu, Y.; Qiu, W.; Zhao, Z.; Li, X.; Yang, H. The microemulsion preparation and high catalytic performance of mesoporous NiO nanorods and nanocubes for toluene combustion. *Chem. Eng. J.* **2013**, *219*, 200–208. [CrossRef]

62. Ye, Y.; Zhao, Y.; Ni, L.; Jiang, K.; Tong, G.; Zhao, Y.; Teng, B. Facile synthesis of unique NiO nanostructures for efficiently catalytic conversion of CH_4 at low temperature. *Appl. Surf. Sci.* **2016**, *362*, 20–27. [CrossRef]

63. Kim, H.-J.; Lee, J.-H. Highly sensitive and selective gas sensors using p-type oxide semiconductors: Overview. *Sens. Actuators B Chem.* **2014**, *192*, 607–627. [CrossRef]

64. Mokoena, T.P.; Swart, H.C.; Motaung, D.E. A review on recent progress of p-type nickel oxide based gas sensors: Future perspectives. *J. Alloy. Compd.* **2019**, *805*, 267–294. [CrossRef]

65. Lin, L.; Liu, T.; Miao, B.; Zeng, W. Hydrothermal fabrication of uniform hexagonal NiO nanosheets: Structure, growth and response. *Mater. Lett.* **2013**, *102–103*, 43–46. [CrossRef]

66. Miao, R.; Zeng, W.; Gao, Q. Hydrothermal synthesis of novel NiO nanoflowers assisted with CTAB and SDS respectively and their gas-sensing properties. *Mater. Lett.* **2017**, *186*, 175–177. [CrossRef]

67. Liu, B.; Yang, H.; Zhao, H.; An, L.; Zhang, L.; Shi, R.; Wang, L.; Bao, L.; Chen, Y. Synthesis and enhanced gas-sensing properties of ultralong NiO nanowires assembled with NiO nanocrystals. *Sens. Actuators B Chem.* **2011**, *156*, 251–262. [CrossRef]

68. Urso, M.; Leonardi, S.G.; Neri, G.; Petralia, S.; Conoci, S.; Priolo, F.; Mirabella, S. Acetone sensing and modelling by low-cost NiO nanowalls. *Mater. Lett.* **2020**, *262*, 127043. [CrossRef]

69. Castro-Hurtado, I.; Malagù, C.; Morandi, S.; Pérez, N.; Mandayo, G.G.; Castaño, E. Properties of NiO sputtered thin films and modeling of their sensing mechanism under formaldehyde atmospheres. *Acta Mater.* **2013**, *61*, 1146–1153. [CrossRef]

70. Cho, N.G.; Hwang, I.-S.; Kim, H.-G.; Lee, J.-H.; Kim, I.-D. Gas sensing properties of p-type hollow NiO hemispheres prepared by polymeric colloidal templating method. *Sens. Actuators B Chem.* **2011**, *155*, 366–371. [CrossRef]

71. Yao, Y.-F.Y. The oxidation of hydrocarbons and CO over metal oxides: II. α-Cr_2O_3. *J. Catal.* **1973**, *28*, 139–149. [CrossRef]

72. Sinha, A.K.; Suzuki, K. Three-Dimensional Mesoporous Chromium Oxide: A Highly Efficient Material for the Elimination of Volatile Organic Compounds. *Angew. Chem. Int. Ed.* **2005**, *44*, 271–273. [CrossRef]

73. Rotter, H.; Landau, M.V.; Carrera, M.; Goldfarb, D.; Herskowitz, M. High surface area chromia aerogel efficient catalyst and catalyst support for ethylacetate combustion. *Appl. Catal. B Environ.* **2004**, *47*, 111–126. [CrossRef]

74. Xia, Y.; Dai, H.; Jiang, H.; Deng, J.; He, H.; Au, C.T. Mesoporous Chromia with Ordered Three-Dimensional Structures for the Complete Oxidation of Toluene and Ethyl Acetate. *Environ. Sci. Technol.* **2009**, *43*, 8355–8360. [CrossRef]

75. Bumajdad, A.; Al-Ghareeb, S.; Madkour, M.; Al Sagheer, F. Non-noble, efficient catalyst of unsupported α-Cr_2O_3 nanoparticles for low temperature CO Oxidation. *Sci. Rep.* **2017**, *7*, 14788. [CrossRef]

76. Rajesh, H.; Ozkan, U.S. Complete oxidation of ethanol, acetaldehyde and ethanol/methanol mixtures over copper oxide and copper-chromium oxide catalysts. *Ind. Eng. Chem. Res.* **1993**, *32*, 1622–1630. [CrossRef]

77. Miremadi, B.K.; Singh, R.C.; Chen, Z.; Morrison, S.R.; Colbow, K. Chromium oxide gas sensors for the detection of hydrogen, oxygen and nitrogen oxide. *Sens. Actuators B Chem.* **1994**, *21*, 1–4. [CrossRef]

78. An, G.; Zhang, Y.; Liu, Z.; Miao, Z.; Han, B.; Miao, S.; Li, J. Preparation of porous chromium oxide nanotubes using carbon nanotubes as templates and their application as an ethanol sensor. *Nanotechnology* **2007**, *19*, 035504. [CrossRef]

79. Ma, H.; Xu, Y.; Rong, Z.; Cheng, X.; Gao, S.; Zhang, X.; Zhao, H.; Huo, L. Highly toluene sensing performance based on monodispersed Cr_2O_3 porous microspheres. *Sens. Actuators B Chem.* **2012**, *174*, 325–331. [CrossRef]

80. Ding, C.; Ma, Y.; Lai, X.; Yang, Q.; Xue, P.; Hu, F.; Geng, W. Ordered Large-Pore Mesoporous Cr_2O_3 with Ultrathin Framework for Formaldehyde Sensing. *ACS Appl. Mater. Interfaces* **2017**, *9*, 18170–18177. [CrossRef]

81. Pokhrel, S.; Simion, C.E.; Quemener, V.; Bârsan, N.; Weimar, U. Investigations of conduction mechanism in Cr_2O_3 gas sensing thick films by ac impedance spectroscopy and work function changes measurements. *Sens. Actuators B Chem.* **2008**, *133*, 78–83. [CrossRef]

82. Barsan, N.; Simion, C.; Heine, T.; Pokhrel, S.; Weimar, U. Modeling of sensing and transduction for p-type semiconducting metal oxide based gas sensors. *J. Electroceramics* **2010**, *25*, 11–19. [CrossRef]

83. Raymond, M.V.; Smyth, D.M. Defects and charge transport in perovskite ferroelectrics. *J. Phys. Chem. Solids* **1996**, *57*, 1507–1511. [CrossRef]

84. Ji, Q.; Bi, L.; Zhang, J.; Cao, H.; Zhao, X.S. The role of oxygen vacancies of ABO_3 perovskite oxides in the oxygen reduction reaction. *Energy Environ. Sci.* **2020**, *13*, 1408–1428. [CrossRef]

85. Wu, Y.; Yu, T.; Dou, B.-S.; Wang, C.-X.; Xie, X.-F.; Yu, Z.-L.; Fan, S.-R.; Fan, Z.-R.; Wang, L.-C. A comparative study on perovskite-type mixed oxide catalysts $A'_xA_{1-x}BO_{3-\lambda}$ (A' = Ca, Sr, A = La, B = Mn, Fe, Co) for NH_3 oxidation. *J. Catal.* **1989**, *120*, 88–107. [CrossRef]

86. Wells, A.F. *Structural Inorganic Chemistry*, 3rd ed.; Clarendon Press: Oxford, UK, 1962; pp. 494–499.

87. Zhu, J.; Li, H.; Zhong, L.; Xiao, P.; Xu, X.; Yang, X.; Zhao, Z.; Li, J. Perovskite Oxides: Preparation, Characterizations, and Applications in Heterogeneous Catalysis. *ACS Catal.* **2014**, *4*, 2917–2940. [CrossRef]

88. Bhalla, A.S.; Guo, R.; Roy, R. The perovskite structure—A review of its role in ceramic science and technology. *Mater. Res. Innov.* **2000**, *4*, 3–26. [CrossRef]

89. Evans, H.A.; Wu, Y.; Seshadri, R.; Cheetham, A.K. Perovskite-related ReO_3-type structures. *Nat. Rev. Mater.* **2020**, *5*, 196–213. [CrossRef]

90. Sebastian, M.T. ABO3 Type Perovskites. In *Dielectric Materials for Wireless Communication*; Sebastian, M.T., Ed.; Elsevier: Amsterdam, The Netherlands, 2008; pp. 161–203. [CrossRef]

91. Bashan, V.; Ust, Y. Perovskite catalysts for methane combustion: Applications, design, effects for reactivity and partial oxidation. *Int. J. Energy Res.* **2019**, *43*, 7755–7789. [CrossRef]

92. Hwang, J.; Rao, R.R.; Giordano, L.; Katayama, Y.; Yu, Y.; Shao-Horn, Y. Perovskites in catalysis and electrocatalysis. *Science* **2017**, *358*, 751. [CrossRef] [PubMed]

93. Labhasetwar, N.; Saravanan, G.; Megarajan, S.K.; Manwar, N.; Khobragade, R.; Doggali, P.; Grasset, F. Perovskite-type catalytic materials for environmental applications. *Sci. Technol. Adv. Mater.* **2015**, *16*, 036002. [CrossRef]

94. Fierro, J.L.G. Structure and composition of perovskite surface in relation to adsorption and catalytic properties. *Catal. Today* **1990**, *8*, 153–174. [CrossRef]

95. Tejuca, L.G.; Fierro, J.L.G.; Tascón, J.M.D. Structure and Reactivity of Perovskite-Type Oxides. In *Advances in Catalysis*; Eley, D.D., Pines, H., Weisz, P.B., Eds.; Academic Press: Cambridge, MA, USA, 1989; Volume 36, pp. 237–328.

96. Misono, M. Chapter 3—Catalysis of Perovskite and Related Mixed Oxides. In *Studies in Surface Science and Catalysis*; Misono, M., Ed.; Elsevier: Amsterdam, The Netherlands, 2013; Volume 176, pp. 67–95.

97. Parravano, G. Catalytic Activity of Lanthanum and Strontium Manganite. *J. Am. Chem. Soc.* **1953**, *75*, 1497–1498. [CrossRef]

98. Voorhoeve, R.J.H. Perovskite-Related Oxides as Oxidation—Reduction Catalysts. In *Advanced Materials in Catalysis*; Burton, J.J., Garten, R.L., Eds.; Academic Press: Cambridge, MA, USA, 1977; pp. 129–180. [CrossRef]

99. Dowden, D.A. Crystal and Ligand Field Models of Solid Catalysts. *Catal. Rev.* **1972**, *5*, 1–32. [CrossRef]

100. Karki, S.B.; Hona, R.K.; Ramezanipour, F. Effect of Structure on Sensor Properties of Oxygen-Deficient Perovskites, $A_2BB'O_5$ (A = Ca, Sr; B = Fe; B′ = Fe, Mn) for Oxygen, Carbon Dioxide and Carbon Monoxide Sensing. *J. Electron. Mater.* **2020**, *49*, 1557–1567. [CrossRef]

101. Nakamura, T.; Misono, M.; Yoneda, Y. Catalytic Properties of Perovskite-type Mixed Oxides, $La_{1-x}Sr_xCoO_3$. *Bull. Chem. Soc. Jpn.* **1982**, *55*, 394–399. [CrossRef]

102. Taguchi, H.; Yamasaki, S.; Itadani, A.; Yosinaga, M.; Hirota, K. CO oxidation on perovskite-type $LaCoO_3$ synthesized using ethylene glycol and citric acid. *Catal. Commun.* **2008**, *9*, 1913–1915. [CrossRef]

103. Panich, N.M.; Pirogova, G.N.; Korosteleva, R.I.; Voronin, Y.V. Oxidation of CO and hydrocarbons over perovskite-type complex oxides. *Russ. Chem. Bull.* **1999**, *48*, 694–697. [CrossRef]

104. Viswanathan, B. CO Oxidation and NO Reduction on Perovskite Oxides. *Catal. Rev.* **1992**, *34*, 337–354. [CrossRef]

105. Royer, S.; Duprez, D.; Can, F.; Courtois, X.; Batiot-Dupeyrat, C.; Laassiri, S.; Alamdari, H. Perovskites as Substitutes of Noble Metals for Heterogeneous Catalysis: Dream or Reality. *Chem. Rev.* **2014**, *114*, 10292–10368. [CrossRef]

106. Fergus, J.W. Perovskite oxides for semiconductor-based gas sensors. *Sens. Actuators B Chem.* **2007**, *123*, 1169–1179. [CrossRef]

107. Zhang, L.; Hu, J.; Song, P.; Qin, H.; An, K.; Wang, X.; Jiang, M. CO-sensing properties of perovskite $La_{0.68}Pb_{0.32}FeO_3$ nano-materials. *Sens. Actuators B Chem.* **2006**, *119*, 315–318. [CrossRef]

108. Song, P.; Wang, Q.; Yang, Z. The effects of annealing temperature on the CO-sensing property of perovskite $La_{0.8}Pb_{0.2}Fe_{0.8}Cu_{0.2}O_3$ nanoparticles. *Sens. Actuators B Chem.* **2009**, *141*, 109–115. [CrossRef]

109. Giang, H.T.; Duy, H.T.; Ngan, P.Q.; Thai, G.H.; Toan, N.N. Hydrocarbon gas sensing of nano-crystalline perovskite oxides $LnFeO_3$ (Ln=La, Nd and Sm). *Sens. Actuators B Chem.* **2011**, *158*, 246–251. [CrossRef]

110. Lee, Y.N.; Lago, R.M.; Fierro, J.L.G.; Cortés, V.; Sapiña, F.; Martínez, E. Surface properties and catalytic performance for ethane combustion of $La_{1-x}K_xMnO_{3+\delta}$ perovskites. *Appl. Catal. A Gen.* **2001**, *207*, 17–24. [CrossRef]

111. Alifanti, M.; Bueno, G.; Parvulescu, V.; Parvulescu, V.I.; Corberán, V.C. Oxidation of ethane on high specific surface $SmCoO_3$ and $PrCoO_3$ perovskites. *Catal. Today* **2009**, *143*, 309–314. [CrossRef]

112. Nitadori, T.; Kurihara, S.; Misono, M. Catalytic properties of $La_{1-x}A'_xMnO_3$ (A' = Sr, Ce, Hf). *J. Catal.* **1986**, *98*, 221–228. [CrossRef]

113. Merino, N.A.; Barbero, B.P.; Grange, P.; Cadús, L.E. $La_{1-x}Ca_xCoO_3$ perovskite-type oxides: Preparation, characterisation, stability, and catalytic potentiality for the total oxidation of propane. *J. Catal.* **2005**, *231*, 232–244. [CrossRef]

114. Asada, T.; Kayama, T.; Kusaba, H.; Einaga, H.; Teraoka, Y. Preparation of alumina-supported $LaFeO_3$ catalysts and their catalytic activity for propane combustion. *Catal. Today* **2008**, *139*, 37–42. [CrossRef]

115. Sui, Z.-J.; Vradman, L.; Reizner, I.; Landau, M.V.; Herskowitz, M. Effect of preparation method and particle size on $LaMnO_3$ performance in butane oxidation. *Catal. Commun.* **2011**, *12*, 1437–1441. [CrossRef]

116. Szabo, V.; Bassir, M.; Gallot, J.E.; Van Neste, A.; Kaliaguine, S. Perovskite-type oxides synthesised by reactive grinding: Part III. Kinetics of n-hexane oxidation over $LaCo_{(1-x)}Fe_xO_3$. *Appl. Catal. B Environ.* **2003**, *42*, 265–277. [CrossRef]

117. Levasseur, B.; Kaliaguine, S. Methanol oxidation on $LaBO_3$ (B = Co, Mn, Fe) perovskite-type catalysts prepared by reactive grinding. *Appl. Catal. A Gen.* **2008**, *343*, 29–38. [CrossRef]

118. Pecchi, G.; Reyes, P.; Zamora, R.; Cadús, L.E.; Fierro, J.L.G. Surface properties and performance for VOCs combustion of $LaFe_{1-y}Ni_yO_3$ perovskite oxides. *J. Solid State Chem.* **2008**, *181*, 905–912. [CrossRef]

119. Najjar, H.; Batis, H. La–Mn perovskite-type oxide prepared by combustion method: Catalytic activity in ethanol oxidation. *Appl. Catal. A Gen.* **2010**, *383*, 192–201. [CrossRef]

120. Białobok, B.; Trawczyński, J.; Miśta, W.; Zawadzki, M. Ethanol combustion over strontium- and cerium-doped $LaCoO_3$ catalysts. *Appl. Catal. B Environ.* **2007**, *72*, 395–403. [CrossRef]

121. Stege, W.P.; Cadús, L.E.; Barbero, B.P. $La_{1-x}Ca_xMnO_3$ perovskites as catalysts for total oxidation of volatile organic compounds. *Catal. Today* **2011**, *172*, 53–57. [CrossRef]

122. Spinicci, R.; Faticanti, M.; Marini, P.; De Rossi, S.; Porta, P. Catalytic activity of $LaMnO_3$ and $LaCoO_3$ perovskites towards VOCs combustion. *J. Mol. Catal. A Chem.* **2003**, *197*, 147–155. [CrossRef]

123. Qin, J.; Cui, Z.; Yang, X.; Zhu, S.; Li, Z.; Liang, Y. Three-dimensionally ordered macroporous $La_{1-x}Mg_xFeO_3$ as high performance gas sensor to methanol. *J. Alloy. Compd.* **2015**, *635*, 194–202. [CrossRef]

124. Obayashi, H.; Sakurai, Y.; Gejo, T. Perovskite-type oxides as ethanol sensors. *J. Solid State Chem.* **1976**, *17*, 299–303. [CrossRef]

125. Ge, X.; Liu, Y.; Liu, X. Preparation and gas-sensitive properties of $LaFe_{1-y}Co_yO_3$ semiconducting materials. *Sens. Actuators B Chem.* **2001**, *79*, 171–174. [CrossRef]

126. Song, P.; Qin, H.; Zhang, L.; An, K.; Lin, Z.; Hu, J.; Jiang, M. The structure, electrical and ethanol-sensing properties of $La^{1-x}Pb_xFeO_3$ perovskite ceramics with x ≤ 0.3. *Sens. Actuators B Chem.* **2005**, *104*, 312–316. [CrossRef]

127. Cao, K.; Cao, E.; Zhang, Y.; Hao, W.; Sun, L.; Peng, H. The influence of nonstoichiometry on electrical transport and ethanol sensing characteristics for nanocrystalline $LaFe_xO_{3-\delta}$ sensors. *Sens. Actuators B Chem.* **2016**, *230*, 592–599. [CrossRef]

128. Xiang, J.; Chen, X.; Zhang, X.; Gong, L.; Zhang, Y.; Zhang, K. Preparation and characterization of Ba-doped $LaFeO_3$ nanofibers by electrospinning and their ethanol sensing properties. *Mater. Chem. Phys.* **2018**, *213*, 122–129. [CrossRef]

129. Hao, P.; Qu, G.-M.; Song, P.; Yang, Z.-X.; Wang, Q. Synthesis of Ba-doped porous $LaFeO_3$ microspheres with perovskite structure for rapid detection of ethanol gas. *Rare Met.* **2021**, *40*, 1651–1661. [CrossRef]

130. Einaga, H.; Hyodo, S.; Teraoka, Y. Complete Oxidation of Benzene Over Perovskite-Type Oxide Catalysts. *Top. Catal.* **2010**, *53*, 629–634. [CrossRef]

131. Deng, J.; Zhang, L.; Dai, H.; He, H.; Au, C.T. Hydrothermally fabricated single-crystalline strontium-substituted lanthanum manganite microcubes for the catalytic combustion of toluene. *J. Mol. Catal. A Chem.* **2009**, *299*, 60–67. [CrossRef]

132. Blasin-Aubé, V.; Belkouch, J.; Monceaux, L. General study of catalytic oxidation of various VOCs over $La_{0.8}Sr_{0.2}MnO_{3+x}$ perovskite catalyst—influence of mixture. *Appl. Catal. B Environ.* **2003**, *43*, 175–186. [CrossRef]

133. Deng, J.; Zhang, L.; Dai, H.; He, H.; Au, C.T. Strontium-Doped Lanthanum Cobaltite and Manganite: Highly Active Catalysts for Toluene Complete Oxidation. *Ind. Eng. Chem. Res.* **2008**, *47*, 8175–8183. [CrossRef]

134. Niu, J.; Deng, J.; Liu, W.; Zhang, L.; Wang, G.; Dai, H.; He, H.; Zi, X. Nanosized perovskite-type oxides $La_{1-x}Sr_xMO_{3-\delta}$ (M=Co, Mn; x=0, 0.4) for the catalytic removal of ethylacetate. *Catal. Today* **2007**, *126*, 420–429. [CrossRef]

135. Xiao, H.; Xue, C.; Song, P.; Li, J.; Wang, Q. Preparation of porous $LaFeO_3$ microspheres and their gas-sensing property. *Appl. Surf. Sci.* **2015**, *337*, 65–71. [CrossRef]

136. Yao, P.-J.; Wang, J.; Chu, W.-L.; Hao, Y.-W. Preparation and characterization of La$_{1-x}$Sr$_x$FeO$_3$ materials and their formaldehyde gas-sensing properties. *J. Mater. Sci.* **2013**, *48*, 441–450. [CrossRef]

137. Menesklou, W.; Schreiner, H.-J.; Härdtl, K.H.; Ivers-Tiffée, E. High temperature oxygen sensors based on doped SrTiO$_3$. *Sens. Actuators B Chem.* **1999**, *59*, 184–189. [CrossRef]

138. Shellaiah, M.; Sun, K.W. Review on Sensing Applications of Perovskite Nanomaterials. *Chemosensors* **2020**, *8*, 55. [CrossRef]

139. Bulemo, P.M.; Kim, I.-D. Recent advances in ABO$_3$ perovskites: Their gas-sensing performance as resistive-type gas sensors. *J. Korean Ceram. Soc.* **2020**, *57*, 24–39. [CrossRef]

140. Queraltó, A.; Graf, D.; Frohnhoven, R.; Fischer, T.; Vanrompay, H.; Bals, S.; Bartasyte, A.; Mathur, S. LaFeO$_3$ Nanofibers for High Detection of Sulfur-Containing Gases. *ACS Sustain. Chem. Eng.* **2019**, *7*, 6023–6032. [CrossRef]

141. Ma, X.-H.; Li, H.-Y.; Kweon, S.-H.; Jeong, S.-Y.; Lee, J.-H.; Nahm, S. Highly Sensitive and Selective PbTiO$_3$ Gas Sensors with Negligible Humidity Interference in Ambient Atmosphere. *ACS Appl. Mater. Interfaces* **2019**, *11*, 5240–5246. [CrossRef] [PubMed]

142. Alharbi, A.A.; Sackmann, A.; Weimar, U.; Bârsan, N. Acetylene- and Ethylene-Sensing Mechanism for LaFeO$_3$-Based Gas Sensors: Operando Insights. *J. Phys. Chem. C* **2020**, *124*, 7317–7326. [CrossRef]

143. Mirzaei, A.; Hashemi, B.; Janghorban, K. α-Fe$_2$O$_3$ based nanomaterials as gas sensors. *J. Mater. Sci. Mater. Electron.* **2016**, *27*, 3109–3144. [CrossRef]

144. Cuong, N.D.; Khieu, D.Q.; Hoa, T.T.; Quang, D.T.; Viet, P.H.; Dai Lam, T.; Hoa, N.D.; Van Hieu, N. Facile synthesis of α-Fe$_2$O$_3$ nanoparticles for high-performance CO gas sensor. *Mater. Res. Bull.* **2015**, *68*, 302–307. [CrossRef]

145. Xue, Y.; Wang, Y. A review of the α-Fe$_2$O$_3$ (hematite) nanotube structure: Recent advances in synthesis, characterization, and applications. *Nanoscale* **2020**, *12*, 10912–10932. [CrossRef]

146. Wang, P.; Sui, L.; Yu, H.; Zhang, X.; Cheng, X.; Gao, S.; Zhao, H.; Huo, L.; Xu, Y.; Wu, H. Monodispersed hollow α-Fe$_2$O$_3$ ellipsoids via [C$_{12}$mim][PF$_6$]-assistant synthesis and their excellent n-butanol gas-sensing properties. *Sens. Actuators B Chem.* **2021**, *326*, 128796. [CrossRef]

147. Ma, T.; Zheng, L.; Zhao, Y.; Xu, Y.; Zhang, J.; Liu, X. Highly Porous Double-Shelled Hollow Hematite Nanoparticles for Gas Sensing. *ACS Appl. Nano Mater.* **2019**, *2*, 2347–2357. [CrossRef]

148. Wu, Z.; Li, Z.; Li, H.; Sun, M.; Han, S.; Cai, C.; Shen, W.; Fu, Y. Ultrafast Response/Recovery and High Selectivity of the H$_2$S Gas Sensor Based on α-Fe$_2$O$_3$ Nano-Ellipsoids from One-Step Hydrothermal Synthesis. *ACS Appl. Mater. Interfaces* **2019**, *11*, 12761–12769. [CrossRef]

149. Tian, K.; Wang, X.-X.; Yu, Z.-Y.; Li, H.-Y.; Guo, X. Hierarchical and Hollow Fe$_2$O$_3$ Nanoboxes Derived from Metal–Organic Frameworks with Excellent Sensitivity to H$_2$S. *ACS Appl. Mater. Interfaces* **2017**, *9*, 29669–29676. [CrossRef] [PubMed]

150. Li, Z.; Lin, Z.; Wang, N.; Huang, Y.; Wang, J.; Liu, W.; Fu, Y.; Wang, Z. Facile synthesis of α-Fe$_2$O$_3$ micro-ellipsoids by surfactant-free hydrothermal method for sub-ppm level H$_2$S detection. *Mater. Des.* **2016**, *110*, 532–539. [CrossRef]

151. Li, P.; Miser, D.E.; Rabiei, S.; Yadav, R.T.; Hajaligol, M.R. The removal of carbon monoxide by iron oxide nanoparticles. *Appl. Catal. B Environ.* **2003**, *43*, 151–162. [CrossRef]

152. Xiong, Y.; Li, Z.; Li, X.; Hu, B.; Xie, Y. Thermally Stable Hematite Hollow Nanowires. *Inorg. Chem.* **2004**, *43*, 6540–6542. [CrossRef]

153. Zheng, Y.; Cheng, Y.; Wang, Y.; Bao, F.; Zhou, L.; Wei, X.; Zhang, Y.; Zheng, Q. Quasicubic α-Fe$_2$O$_3$ Nanoparticles with Excellent Catalytic Performance. *J. Phys. Chem. B* **2006**, *110*, 3093–3097. [CrossRef]

154. Barbosa, A.L.; Herguido, J.; Santamaria, J. Methane combustion over unsupported iron oxide catalysts. *Catal. Today* **2001**, *64*, 43–50. [CrossRef]

155. Dobosz, J.; Zawadzki, M. Total oxidation of lean propane over α-Fe$_2$O$_3$ using microwaves as an energy source. *React. Kinet. Mech. Catal.* **2015**, *114*, 157–172. [CrossRef]

156. Solsona, B.; García, T.; Sanchis, R.; Soriano, M.D.; Moreno, M.; Rodríguez-Castellón, E.; Agouram, S.; Dejoz, A.; Nieto, J.L. Total oxidation of VOCs on mesoporous iron oxide catalysts: Soft chemistry route versus hard template method. *Chem. Eng. J.* **2016**, *290*, 273–281. [CrossRef]

157. Parkinson, G.S. Iron oxide surfaces. *Surf. Sci. Rep.* **2016**, *71*, 272–365. [CrossRef]

158. Guerrero-Pérez, M.O. Supported, bulk and bulk-supported vanadium oxide catalysts: A short review with an historical perspective. *Catal. Today* **2017**, *285*, 226–233. [CrossRef]

159. Wachs, I.E. Catalysis science of supported vanadium oxide catalysts. *Dalton Trans.* **2013**, *42*, 11762–11769. [CrossRef] [PubMed]

160. Gannoun, C.; Delaigle, R.; Ghorbel, A.; Gaigneaux, E.M. V$_2$O$_5$/TiO$_2$ and V$_2$O$_5$/TiO$_2$–SO$_4^{2-}$ catalysts for the total oxidation of chlorobenzene: One-step sol–gel preparation vs. two-step impregnation. *Catal. Sci. Technol.* **2019**, *9*, 2344–2350. [CrossRef]

161. Wang, J.; Wang, X.; Liu, X.; Zhu, T.; Guo, Y.; Qi, H. Catalytic oxidation of chlorinated benzenes over V$_2$O$_5$/TiO$_2$ catalysts: The effects of chlorine substituents. *Catal. Today* **2015**, *241*, 92–99. [CrossRef]

162. Moon, S.W.; Lee, G.-D.; Park, S.S.; Hong, S.-S. Catalytic combustion of chlorobenzene over V$_2$O$_5$/TiO$_2$ catalysts prepared by the precipitation-deposition method. *React. Kinet. Catal. Lett.* **2004**, *82*, 303–310. [CrossRef]

163. Debecker, D.P.; Bouchmella, K.; Delaigle, R.; Eloy, P.; Poleunis, C.; Bertrand, P.; Gaigneaux, E.M.; Mutin, P.H. One-step non-hydrolytic sol-gel preparation of efficient V$_2$O$_5$-TiO$_2$ catalysts for VOC total oxidation. *Appl. Catal. B Environ.* **2010**, *94*, 38–45. [CrossRef]

164. Guerrero-Pérez, M.O. V-Containing Mixed Oxide Catalysts for Reduction–Oxidation-Based Reactions with Environmental Applications: A Short Review. *Catalysts* **2018**, *8*, 564. [CrossRef]

165. Haber, J. Fifty years of my romance with vanadium oxide catalysts. *Catal. Today* **2009**, *142*, 100–113. [CrossRef]

166. Grzybowska-Swierkosz, B. Vanadia-titania catalysts for oxidation of o-xylene and other hydrocarbons. *Appl. Catal. A Gen.* **1997**, *157*, 263–310. [CrossRef]

167. Bond, G.C.; Tahir, S.F. Vanadium oxide monolayer catalysts Preparation, characterization and catalytic activity. *Appl. Catal.* **1991**, *71*, 1–31. [CrossRef]

168. Deo, G.; Wachs, I.E. Reactivity of Supported Vanadium Oxide Catalysts: The Partial Oxidation of Methanol. *J. Catal.* **1994**, *146*, 323–334. [CrossRef]

169. Carrero, C.A.; Schloegl, R.; Wachs, I.E.; Schomaecker, R. Critical Literature Review of the Kinetics for the Oxidative Dehydrogenation of Propane over Well-Defined Supported Vanadium Oxide Catalysts. *ACS Catal.* **2014**, *4*, 3357–3380. [CrossRef]

170. Pan, J.-B.; Huang, J.-M.; Li, J.-X.; Jiang, Z.-Y.; Lan, J.-L.; Qian, C.; Chen, X.-Z. Ammoxidation of 2-picoline catalyzed by modified V_2O_5/TiO_2. *Monatsh. Chem.* **2014**, *145*, 1365–1369. [CrossRef]

171. Cavalli, P.; Cavani, F.; Manenti, I.; Trifiro, F. Ammoxidation of alkylaromatics over V_2O_5/TiO_2 catalysts. *Catal. Today* **1987**, *1*, 245–255. [CrossRef]

172. Epifani, M.; Díaz, R.; Force, C.; Comini, E.; Andreu, T.; Zamani, R.R.; Arbiol, J.; Siciliano, P.; Faglia, G.; Morante, J.R. Colloidal Counterpart of the TiO_2-Supported V_2O_5 System: A Case Study of Oxide-on-Oxide Deposition by Wet Chemical Techniques. Synthesis, Vanadium Speciation, and Gas-Sensing Enhancement. *J. Phys. Chem. C* **2013**, *117*, 20697–20705. [CrossRef]

173. Epifani, M.; Comini, E.; Siciliano, P.; Faglia, G.; Morante, J.R. Evidence of catalytic activation of anatase nanocrystals by vanadium oxide surface layer: Acetone and ethanol sensing properties. *Sens. Actuators B Chem.* **2015**, *217*, 193–197. [CrossRef]

174. Ai, M. The oxidation activity and acid-base properties of SnO_2-based binary catalysts: I. The SnO_2 V_2O_5 system. *J. Catal.* **1975**, *40*, 318–326. [CrossRef]

175. Ono, T.; Nakagawa, Y.; Kubokawa, Y. Catalytic Activity of V–Sn Oxides for Oxidation Reactions. *Bull. Chem. Soc. Jpn.* **1981**, *54*, 343–347. [CrossRef]

176. Bordoni, S.; Castellani, F.; Cavani, F.; Trifiro, F.; Gazzano, M. Nature of Vanadium Species in SnO_2-V_2O_5-Based Catalysts-Chemistry of Preparation, Characterization, Thermal-Stability and Reactivity in Ethane Oxidative Dehydrogenation over V-Sn Mixed Oxides. *J. Chem. Soc. Faraday Trans.* **1994**, *90*, 2981–3000. [CrossRef]

177. Cavani, F.; Trifiro, F.; Bartolini, A.; Ghisletti, D.; Nalli, M.; Santucci, A. SnO_2-V_2O_5-based catalysts - Nature of surface species and their activity in o-xylene oxidation. *J. Chem. Soc. Faraday Trans.* **1996**, *92*, 4321–4330. [CrossRef]

178. Glinski, M.; Kijenski, J.; Jelen, T. Monolayer oxide catalysts from alkoxide precursors. 4. Vanadia, titania and stibia on SiO_2, SnO_2, and TiO_2 in 2-propanol oxidation. *React. Kinet. Catal. Lett.* **1997**, *60*, 33–39. [CrossRef]

179. Pillai, S.K.; Gheevarghese, O.; Sugunan, S. Catalytic properties of V_2O_5/SnO_2 towards vapour-phase Beckmann rearrangement of cyclohexanone oxime. *Appl. Catal. A Gen.* **2009**, *353*, 130–136. [CrossRef]

180. Zhang, F.; Wang, X.; Dong, J.; Qin, N.; Xu, J. Selective BTEX sensor based on a SnO_2/V_2O_5 composite. *Sens. Actuators B Chem.* **2013**, *186*, 126–131. [CrossRef]

181. Kim, H.S.; Jin, C.H.; Park, S.H.; Lee, C.M. Structural, luminescent, and NO_2 sensing properties of SnO_2-core/V_2O_5-shell nanorods. *J. Electroceramics* **2013**, *30*, 6–12. [CrossRef]

182. Wang, C.T.; Chen, M.T.; Lai, D.L. Vanadium-Tin Oxide Nanoparticles with Gas-Sensing and Catalytic Activity. *J. Am. Ceram. Soc.* **2011**, *94*, 4471–4477. [CrossRef]

183. Patrono, P.; Laginestra, A.; Ramis, G.; Busca, G. Conversion of 1-Butene over WO_3-TiO_2 Catalysts. *Appl. Catal. A Gen.* **1994**, *107*, 249–266. [CrossRef]

184. Lu, G.; Li, X.; Qu, Z.; Zhao, Q.; Li, H.; Shen, Y.; Chen, G. Correlations of WO_3 species and structure with the catalytic performance of the selective oxidation of cyclopentene to glutaraldehyde on WO_3/TiO_2 catalysts. *Chem. Eng. J.* **2010**, *159*, 242–246. [CrossRef]

185. Ulgen, A.; Hoelderich, W.F. Conversion of glycerol to acrolein in the presence of WO_3/TiO_2 catalysts. *Appl. Catal. A Gen.* **2011**, *400*, 34–38. [CrossRef]

186. Onfroy, T.; Lebarbier, V.; Clet, G.; Houalla, M. Quantitative relationship between the nature of surface species and the catalytic activity of tungsten oxides supported on crystallized titania. *J. Mol. Catal. A Chem.* **2010**, *318*, 1–7. [CrossRef]

187. Epifani, M.; Díaz, R.; Force, C.; Comini, E.; Manzanares, M.; Andreu, T.; Genç, A.; Arbiol, J.; Siciliano, P.; Faglia, G.; et al. Surface Modification of TiO_2 Nanocrystals by WO_x Coating or Wrapping: Solvothermal Synthesis and Enhanced Surface Chemistry. *ACS Appl. Mater. Interfaces* **2015**, *7*, 6898–6908. [CrossRef]

188. Epifani, M.; Comini, E.; Díaz, R.; Genç, A.; Andreu, T.; Siciliano, P.; Morante, J.R. Acetone sensors based on TiO_2 nanocrystals modified with tungsten oxide species. *J. Alloy. Compd.* **2016**, *665*, 345–351. [CrossRef]

189. Staerz, A.; Weimar, U.; Barsan, N. Understanding the Potential of WO_3 Based Sensors for Breath Analysis. *Sensors* **2016**, *16*, 1815. [CrossRef] [PubMed]

190. Reddy, B.M.; Narsimha, K.; Rao, P.K. Effect of Method of Preparation on the Reactivity of Molybdena Supported on Titania. *Langmuir* **1991**, *7*, 1551–1553. [CrossRef]

191. Segawa, K.; Soeya, T.; Kim, D.S. Supported Molybdenum Oxide Catalyst. Structure and Chemistry of Oxidized, Reduced, and Sulfided Surfaces. *J. Jpn. Pet. Inst.* **1990**, *33*, 347–359. [CrossRef]

192. Hu, H.; Wachs, I.E. Catalytic Properties of Supported Molybdenum Oxide Catalysts—In-Situ Raman and Methanol Oxidation Studies. *J. Phys. Chem.* **1995**, *99*, 10911–10922. [CrossRef]

193. Matsuoka, Y.; Niwa, M.; Murakami, Y. Morphology of molybdena supported on various oxides and its activity for methanol oxidation. *J. Phys. Chem.* **1990**, *94*, 1477–1482. [CrossRef]

194. Brückman, K.; Grzybowska, B.; Che, M.; Tatibouët, J.M. Methanol oxidation on MoO$_3$/TiO$_2$ catalysts. *Appl. Catal. A Gen.* **1993**, *96*, 279–288. [CrossRef]

195. Zhang, W.; Desikan, A.; Oyama, S.T. Effect of Support in Ethanol Oxidation on Molybdenum Oxide. *J. Phys. Chem.* **1995**, *99*, 14468–14476. [CrossRef]

196. Shimada, H.; Sato, T.; Yoshimura, Y.; Hiraishi, J.; Nishijima, A. Support effect on the catalytic activity and properties of sulfided molybdenum catalysts. *J. Catal.* **1988**, *110*, 275–284. [CrossRef]

197. Chary, K.V.R.; Bhaskar, T.; Seela, K.K.; Lakshmi, K.S.; Reddy, K.R. Characterization and reactivity of molybdenum oxide catalysts supported on anatase and rutile polymorphs of titania. *Appl. Catal. A Gen.* **2001**, *208*, 291–305. [CrossRef]

198. Epifani, M.; Kaciulis, S.; Mezzi, A.; Altamura, D.; Giannini, C.; Tang, P.; Morante, J.R.; Arbiol, J.; Siciliano, P.; Comini, E.; et al. Solvothermal Synthesis, Gas-Sensing Properties, and Solar Cell-Aided Investigation of TiO$_2$–MoO$_x$ Nanocrystals. *ChemNanoMat* **2017**, *3*, 798–807. [CrossRef]

199. Pârvulescu, V.I.; Grange, P.; Delmon, B. Catalytic removal of NO. *Catal. Today* **1998**, *46*, 233–316. [CrossRef]

200. Barsan, N.; Weimar, U. Conduction Model of Metal Oxide Gas Sensors. *J. Electroceramics* **2001**, *7*, 143–167. [CrossRef]

201. Mars, P.; van Krevelen, D.W. Oxidations carried out by means of vanadium oxide catalysts. *Chem. Eng. Sci.* **1954**, *3*, 41–59. [CrossRef]

202. Doornkamp, C.; Ponec, V. The universal character of the Mars and Van Krevelen mechanism. *J. Mol. Catal. A Chem.* **2000**, *162*, 19–32. [CrossRef]

203. Degler, D.; Wicker, S.; Weimar, U.; Barsan, N. Identifying the Active Oxygen Species in SnO$_2$ Based Gas Sensing Materials: An Operando IR Spectrsocopy Study. *J. Phys. Chem. C* **2015**, *119*, 11792–11799. [CrossRef]